Conjugated Aromatic Polyimines. 2. Synthesis, Structure, and Properties of New Aromatic Polyazomethines

Chen-Jen Yang and Samson A. Jenekhe*

Department of Chemical Engineering and Center for Photoinduced Charge Transfer, University of Rochester, Rochester, New York 14627-0166

Received August 29, 1994®

ABSTRACT: A series of 20 conjugated aromatic polyimines, containing *p*-phenylene, *p*-biphenylene, *p*-terphenylene, 4,4′-stilbene, and 1,5-naphthalene linkages in the backbone and various electron-donating and electron-withdrawing side-group substitutions, has been synthesized, characterized, and used to investigate the effects of molecular structure on the electronic structure and properties of conjugated polymers. Soluble gallium trichloride or diaryl phosphate complexes of the aromatic polyimines in organic solvents facilitated their solution spectroscopic (^{1}H NMR, UV−vis) characterization and their processing into thin films and coatings. The solid state electronic structure of the polymers was characterized by optical absorption spectroscopy and cyclic voltammetry of thin films. Electrochemical reduction of the aromatic polyimines was reversible with formal potential of −1.93 to −1.52 V (SCE) and 0.22 to 0.86 charge transferred, whereas oxidation was irreversible. The electron affinity and ionization potentials of the series of polymers varied from 2.46 to 2.94 eV and from 4.80 to 5.38 eV, respectively. The associated LUMO and HOMO energy levels are thus tunable by up to 0.48 and 0.58 eV, respectively. The electrochemically and optically determined LUMO−HOMO energy gaps of thin films were very close and in the range of 2.08−2.77 eV; the optical gap of thin films of gallium trichloride or diaryl phosphate complexes of the polyimines was smaller and in the range of 1.66−2.14 eV. The results of this study show that aromatic polyimines are an interesting class of π-conjugated polymers whose electronic structure and properties can be regulated over a wide range by variation in backbone structure, side group substitution, and through intramolecular hydrogen bonding or complexation, backbone planarity.

Introduction

Studies in the synthesis of conjugated polymers and investigation of their electronic, optoelectronic, and nonlinear optical properties constitute a large area of research in contemporary polymer science.[1−8] One of the central goals of these studies is the fundamental understanding of the underlying structure−property relationships that might form the basis for a "molecular engineering" approach to electronic,[1] optoelectronic,[1−6] and photonic[2,7−9] polymers. One class of π-conjugated polymers that is especially attractive for the investigation of structure−property relationships is the aromatic *polyimines* which are also known as *polyazomethines* or *Schiff base polymers*.[10−22] Their synthetic methodology which consists of condensation polymerization of diamines with dialdehydes (or diketones) to give high molecular weight polymers is both simple and versatile considering the relatively mild reaction conditions and the abundant monomer sources.[16] The drawback to investigating the aromatic polyimines in the past was their intractability and insolubility in organic solvents which impeded characterization of their molecular structure and physical properties as well as exploration of their applications outside of high-temperature fibers.[10−22] However, in an earlier paper (part 1 in the series) we reported the successful solubilization of aromatic polyimines in organic solvents via their soluble coordination complexes which facilitated their solution characterization by NMR spectroscopy and processing to films and coatings by spin coating and other techniques.[10] This has opened up opportunities for various studies of the aromatic polyimines. The present paper represents a comprehensive study of aromatic polyimines as conjugated polymers with tunable electronic structures and interesting electroactive and photoactive properties.

Polyimines date back to 1923, when Adams et al. synthesized the first member of this class of polymers by reacting benzidine and *o*-dianisidine with terephthalaldehyde.[11] In 1938, Steinkopf et al. reacted hydrazine with isophthalaldehyde or terephthalaldehyde.[12] The polymerization reaction was done in the molten state and the resulting products were insoluble and infusible.[12] During the 1950s, Marvel et al. tried solution condensation polymerization by reacting aromatic dialdehyde with hydrazine or *o*-phenylenediamine in solvents such as benzene, acetic acid, and dimethylacetamide.[13] However, this solution polymerization scheme was not successful because the product precipitated out of the reaction media rapidly and resulted in a very low molecular weight material.[13] The strong interest in thermally stable polymers for aircraft application during the late 1960s and the early 1970s led to a systematic study of the synthesis of aromatic polyimines by D'Alelio et al., who reported various reaction schemes, including the melt polymerization of aromatic dialdehydes with aromatic diamines and the carbonyl-, amine-, and bis-exchange reactions of Schiff base molecules.[14] Although the exchange reactions provided an interesting new synthetic route to the aromatic polyimines by changing the reaction byproduct from water to benzaldehyde, aniline, and benzylidine for carbonyl-, amine-, and bis-exchange reactions, respectively, the molecular structures of the resulting polymers were questionable due to the very high reaction temperatures (>400 °C) used in the polymerizations.[14] The infrared spectra of D'Alelio's polymers were different from those of aromatic polyimines synthesized by solution polymerization; the IR spectra exhibited a broad and featureless band in the 900−1600 cm^{-1} spectral range, suggesting that side reactions had occurred in the high-temperature polymerizations.[15] Morgan et al. used derivatization, in which one of the

* To whom correspondence should be addressed.

® Abstract published in *Advance ACS Abstracts,* January 15, 1995.

0024-9297/95/2228-1180$09.00/0 © 1995 American Chemical Society

Chart 1

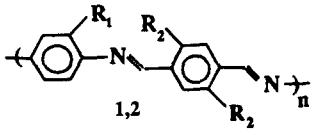

1,2

1a. R_1=H, R_2=H (PPI)
1b. R_1=H, R_2=OCH_3 (PMOPI)
1c. R_1=H, R_2=OH (PHOPI)
1d. R_1=CH_3, R_2=H (PMPI)
2a. R_1=OCH_3, R_2=H (MO-PPI)
2b. R_1=R_2=OCH_3 (P3MOPI)
2c. R_1=OCH_3, R_2=OH (MO-PHOPI)

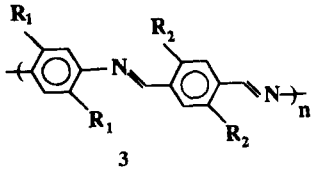

3

3a. R_1=Cl, R_2=H (Cl_2-PPI)
3b. R_1=Cl, R_2=OCH_3 (Cl_2-PMOPI)

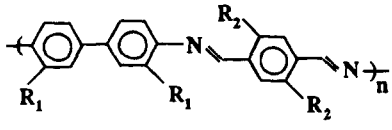

4,5

4a. R_1=R_2=H (PBPI)
4b. R_1=H, R_2=OCH_3 (PBMOPI)
4c. R_1=H, R_2=OH (PBHOPI)
5a. R_1=OCH_3, R_2=H (MO-PBPI)
5b. R_1=R_2=OCH_3 (P4MOBPI)
5c. R_1=OCH_3, R_2=OH (MO-PBHOPI)

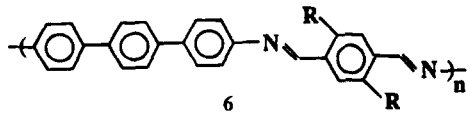

6

6a. R=H (PTPI)
6b. R=OCH_3 (PTMOPI)
6c. R=OH (PTHOPI)

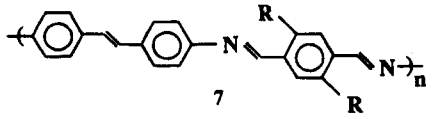

7

7a. R=H (PSPI)
7b. R=OCH_3 (PSMOPI)
7c. R=OH (PSHOPI)

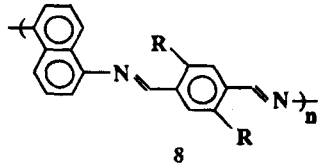

8

8a. R=H (1,5-PNI)
8b. R=OCH_3 (1,5-PMONI)
8c. R=OH (1,5-PHONI)

co-monomers was substituted with methyl or chloro side group, as well as random copolymerization to reduce the melting temperatures of the aromatic polyimines.[16] Consequently, melt polymerization could proceed at lower temperatures (~260 °C) and the resulting polymers were processable into high strength fibers.[16] Another valuable contribution from Morgan's work was the use of mixtures of hexamethylphosphoramide (HMPA) and 1-methyl-2-pyrrolidinone (NMP) as polymerization solvents and water-absorbing lithium chloride in the reaction mixture.[16] High molecular weight polymers were achieved by such a solution polymerization. The molecular weight could further be increased by utilizing a two-stage polymerization scheme in which the product of solution polymerization was further reacted in the molten state.[16] A review of the synthesis of aromatic polyimines and particularly their fiber properties has appeared as a book chapter.[23]

More recent studies of aromatic polyimines include the synthesis of long alkoxy (C_8–C_{18}) side chain derivatives[18,19] which are presumably soluble to some extent in organic solvents and derivatives containing 2,5-bis-(4-aminophenyl)-3,4-diphenylthiophene,[17] fluorene cardo unit,[21a] and trifluoromethyl groups[21b] in the polymer backbone which were also reported to be soluble in organic solvents. Studies of the electrical properties of doped conjugated aromatic polyimines and alkoxy derivatives have been reported. Conductivities in the range of 10^{-6} to 10^{-2} S/cm have been reported.[19,22]

This paper reports our synthesis and detailed characterization of a series of 20 conjugated aromatic polyimines with various backbone and side-group substitution structures. The electronic structure and redox properties of the series of polymers in the solid state were investigated by electronic absorption spectroscopy and cyclic voltammetry, facilitated by the ready preparation of thin films from their soluble coordination complexes. The molecular structures of the 20 new polymers along with the four previously reported *p*-phenylene-linked polymers (1) are depicted in Chart 1. Although three of the polymers, **4a** (PBPI),[11,14] **5a** (MO-PBPI),[11] and **8a** (1,5-PNI),[22] have been previously synthesized, their structures were not characterized or established. The parent conjugated polyimine is poly(1,4-phenylenemethylidynenitrilo-1,4-phenylenenitrilomethylidyne) (PPI), and the variations of the conjugated polymer backbone include *p*-biphenylene (PBPI), *p*-terphenylene (PTPI), 4,4′-stilbene (PSPI), and 1,5-naphthalene (1,5-PNI) linkages (Chart 1). Monomethoxy, dimethoxy, dihydroxy, and dichloro side-group substitutions on the phenylene rings were also made, resulting in various derivatives with electron-donating and electron-withdrawing side groups.

The diverse backbone and side-group substitution structures of the aromatic polyimines in Chart 1 provide a unique opportunity for exploring structure–property relationships in π-conjugated polymers. We have thus extensively investigated the linear refractive index[9] and the third-order nonlinear optical[7] properties of this series of conjugated polyimines and those studies are reported elsewhere. Availability of the diverse but related series of polymers in Chart 1 has allowed us to correlate the refractive index of conjugated polymers to molecular structure and to formulate a functional group contribution to molar refraction and refractive index which properly accounts for the effects of optical disper-

sion and π-electron conjugation.[9b] Similarly, the nonlinear optical studies by third harmonic generation spectroscopy of the polymers of Chart 1 have revealed large third-order optical nonlinearities that have been correlated with the backbone and side group variations in Chart 1.[7]

Experimental Section

Materials. 2-Methoxy-1,4-phenylenediamine was purified by reprecipitation of the material from methylene chloride solution in hexane, after extraction from an aqueous ammonium hydroxide solution of 2-methoxy-1,4-phenylenediamine sulfate hydrate (95%, Aldrich) with ether. Benzidine (99%, Fluka) was purified by recrystallization from benzene. 4,4'-Diaminostilbene was purified by reprecipitation of the material from acetone solution in hexane, following extraction from an aqueous ammonium hydroxide solution of 4,4'-diaminostilbene dihydrochloride (97%, Aldrich) with ether. 3,3'-Dimethoxybenzidine (97%, Aldrich) was recrystallized from benzene. 1,5-Diaminonaphthalene (>98%, Fluka) was recrystallized from ether. 4,4'-Diamino-*p*-terphenyl (>98%, Lancaster) was used as received. Terephthalaldehyde (98%, Aldrich) was sublimed under vacuum at 100 °C. 2,5-Dimethoxyterephthalaldehyde and 2,5-dihydroxyterephthalaldehyde were prepared by literature methods.[10,24-28] 2,5-Dichloro-1,4-phenylenediamine (98%, Aldrich) was purified by recrystallization from toluene. The polymerization media, hexamethylphosphoramide (HMPA) (99%, Aldrich) and 1-methyl-2-pyrrolidone (NMP) (99+% anhydrous, Aldrich), and the water-absorbing lithium chloride (99%, Aldrich) were used as received. The complexation reagents gallium trichloride (99.99%, Aldrich) and diphenyl phosphate (DPP) (99%, Aldrich) were used as received. The complexation reagent di-*m*-cresyl phosphate (DCP) was synthesized previously.[10]

Preparation of Polymers. All the polymers were prepared by solution condensation polymerization of aromatic diamines with aromatic dialdehydes at room temperature under nitrogen purge.[10,16] The polymers generally precipitated out of the polymerization media during reaction after a reaction time ranging from 24 to 72 h. The polymers were washed repeatedly with water and methanol followed by overnight extraction with refluxing methanol in a Soxhlet apparatus. A brief description of the preparation of each polymer follows.

MO-PPI (2a). 2-Methoxy-1,4-phenylenediamine (0.4203 g, 3.04 mmol) was reacted with terephthalaldehyde (0.4081 g, 3.04 mmol) in 10 mL of 1:1 (by volume) HMPA/NMP containing 0.21 g of LiCl for 24 h to afford an orange powder (0.5411 g, 95% yield).

P3MOPI (2b). 2-Methoxy-1,4-phenylenediamine (0.4032 g, 2.92 mmol) was reacted with 2,5-dimethoxyterephthalaldehyde (0.5666 g, 2.92 mmol) in 10 mL of 1:1 HMPA/NMP containing 0.24 g of LiCl for 48 h to afford an orange powder (0.6345 g, 92% yield).

MO-PHOPI (2c). 2-Methoxy-1,4-phenylenediamine (0.3359 g, 2.43 mmol) was reacted with 2,5-dihydroxyterephthalaldehyde (0.4040 g, 2.43 mmol) in 10 mL of 1:1 HMPA/NMP containing 0.18 g of LiCl for 72 h to afford a dark-red powder (0.5590 g, 86% yield). Anal. Calcd for $(C_{15}H_{12}N_2O_3)_n$: C, 67.16; H, 4.51; N, 10.44; O, 17.89. Found: C, 64.31; H, 4.55; N, 10.04; O, 17.79.

Cl_2-PPI (3a). 2,5-Dichloro-1,4-phenylenediamine (1.5034g, 8.49 mmol) was reacted with terephthalaldehyde (1.1391 g, 8.49 mmol) in 30 mL of 1:1 HMPA/NMP containing 0.4 g of LiCl for 48 h to afford a yellow powder (1.010 g, 43% yield).

Cl_2-PMOPI (3b). 2,5-Dichloro-1,4-phenylenediamine (0.3772 g, 2.13 mmol) was reacted with 2,5-dimethoxyterephthalaldehyde (0.4136 g, 2.13 mmol) in 10 mL of 1:1 HMPA/NMP containing 0.12 g of LiCl for 72 h to afford an orange powder (0.4270 g, 60% yield).

PBPI (4a).[11,14] Benzidine (1.6906 g, 9.18 mmol) was reacted with terephthalaldehyde (1.2308 g, 9.18 mmol) in 30 mL of 1:1 HMPA/NMP containing 0.73 g of LiCl under nitrogen purge at room temperature. The reaction time was 24 h. The polymer is a yellow powder (2.50 g, 96% yield).

PBMOPI (4b). Benzidine (0.3131 g, 1.70 mmol) was reacted with 2,5-dimethoxyterephthalaldehyde (0.3299 g, 1.70 mmol) in 10 mL of 1:1 HMPA/NMP containing 0.16 g of LiCl under nitrogen purge at room temperature. The reaction time was 48 h. The polymer is a yellow powder (0.5131 g, 88% yield).

PBHOPI (4c). Benzidine (0.1342 g, 0.73 mmol) was reacted with 2,5-dihydroxyterephthalaldehyde (0.1209 g, 0.73 mmol) in 10 mL of 1:1 HMPA/NMP containing 0.06 g of LiCl under nitrogen purge at room temperature. The reaction time was 72 h. The polymer is an orange powder (0.1946 g, 85% yield).

MO-PBPI (5a).[11] 3,3'-Dimethoxybenzidine (1.6944 g, 6.94 mmol) was reacted with terephthalaldehyde (0.9303 g, 6.94 mmol) in 20 mL of 1:1 HMPA/NMP containing 0.66 g of LiCl. The reaction time was 24 h. The polymer is a yellow powder (2.1306 g, 91% yield).

P4MOBPI (5b). 3,3'-Dimethoxybenzidine (1.0724 g, 4.39 mmol) was reacted with 2,5-dimethoxyterephthalaldehyde (0.8522 g, 4.39 mmol) in 20 mL of 1:1 HMPA/NMP containing 0.48 g of LiCl for 48 h. The polymer is an orange powder (1.6180 g, 92% yield).

MO-PBHOPI (5c). 3,3'-Dimethoxybenzidine (0.2991 g, 1.22 mmol) was reacted with 2,5-dihydroxyterephthalaldehyde (0.2035 g, 1.22 mmol) in 10 mL of 1:1 HMPA/NMP containing 0.13 g of LiCl for 72 h to afford a red powder (0.4395 g, 96% yield). Anal. calcd. for $(C_{22}H_{18}N_2O_4)_n$: C, 70.58; H, 4.85; N, 7.48; O, 17.09. Found: C, 68.86; H, 4.84; N, 7.43; O, 16.95.

PTPI (6a). 4,4'-Diamino-*p*-terphenyl (0.8519 g, 3.27 mmol) was reacted with terephthaldehyde (0.4389 g, 3.27 mmol) in 30 mL of 1:1 HMPA/NMP containing 0.30 g of LiCl for 24 h to afford a yellow powder (1.0968 g, 94% yield).

PTMOPI (6b). 4,4'-Diamino-*p*-terphenyl (0.4436 g, 1.70 mmol) was reacted with 2,5-dimethoxyterephthalaldehyde (0.3308 g, 1.70 mmole) in 10 mL of 1:1 HMPA/NMP containing 0.19 g of LiCl for 48 h to afford an orange powder (0.6850 g, 96% yield).

PTHOPI (6c). 4,4'-Diamino-*p*-terphenyl (0.2053 g, 0.79 mmol) was reacted with 2,5-dihydroxyterephthalaldehyde (0.1310 g, 0.79 mmol) in 10 mL of 1:1 HMPA/NMP containing 0.10 g of LiCl for 72 h to afford an orange powder (0.2630 g, 85% yield).

PSPI (7a). 4,4'-Diaminostilbene (0.3063 g, 1.46 mmol) was reacted with terephthalaldehyde (0.1955 g, 1.46 mmol) in 10 mL of 1:1 HMPA/NMP containing 0.13 g of LiCl for 24 h to afford an orange powder (0.4189 g, 93% yield). Anal. calcd for $(C_{22}H_{16}N_2)_n$: C, 85.69; H, 5.23; N, 9.08. Found: C, 83.37; H, 5.23; N, 8.63.

PSMOPI (7b). 4,4'-Diaminostilbene (0.2166 g, 1.03 mmol) was reacted with 2,5-dimethoxyterephthalaldehyde (0.2000 g, 1.03 mmol) in 10 mL of 1:1 HMPA/NMP containing 0.10 g of LiCl for 48 h to afford an orange powder (0.3310 g, 87% yield).

PSHOPI (7c). 4,4'-Diaminostilbene (0.1479 g, 0.70 mmol) was reacted with 2,5-dihydroxyterephthalaldehyde (0.1169 g, 0.70 mmol) in 10 mL of 1:1 HMPA/NMP containing 0.06 g of LiCl for 72 h to afford a red powder (0.1820 g, 76% yield).

1,5-PNI (8a).[22] 1,5-Diaminonaphthalene (1.300 g, 8.22 mmol) was reacted with terephthalaldehyde (1.1025 g, 8.22 mmol) in 20 mL of 1:1 HMPA/NMP containing 0.60 g of LiCl for 24 h to afford a yellow powder (1.7505 g, 83% yield).

1,5-PMONI (8b). 1,5-Diaminonaphthalene (0.1162 g, 0.73 mmol) was reacted with 2,5-dimethoxyterephthalaldehyde (0.1220 g, 0.73 mmol) in 10 mL of 1:1 HMPA/NMP containing 0.06 g of LiCl for 72 h to afford an orange powder (0.3844 g, 76% yield).

1,5-PHONI (8c). 1,5-Diaminonaphthalene (0.1162 g, 0.73 mmol) was reacted with 2,5-dihydroxyterephthalaldehyde (0.1220 g, 0.73 mmol) in 10 mL of 1:1 HMPA/NMP containing 0.06 g of LiCl for 72 h to afford an orange powder (0.1525 g, 72% yield).

Preparation of Complexes and Thin Films. The diphenyl phosphate (DPP) complexes were prepared by the same procedures as the preparation of the DCP (DCP = di-*m*-cresyl phosphate) complexes of other conjugated aromatic polyimines in our earlier studies.[10] The dihydroxy-substituted polymers do not form complexes with DPP or DCP due to the intramolecular hydrogen bonding between imine nitrogen and the

hydroxyl groups.[10] Except for PBPI, PTPI, and PSPI in which a higher molar ratio of DPP to imine (CH=N) nitrogen is required for solubilization, the molar ratio of DPP to imine nitrogen on polymer chain can be varied from 0.5:1 to 1:1 to afford soluble complexes in *m*-cresol. The 1:1 molar ratio was used to prepare stoichiometric solid complexes for studying their optical absorption spectra. For the purpose of preparing optical-quality thin films of the pure polymers, the 0.5:1 molar ratio was used because the 0.5:1 complexes have been shown to be completely amorphous, in contrast to the semicrystalline 1:1 complexes.[29]

All the conjugated aromatic polyimines in the present study can also form soluble complexes with $GaCl_3$ in nitromethane, nitroethane, and nitrobenzene. The preparation procedures for the $GaCl_3$ complexes of the polyimines were similar to that used for other polymers.[10,30-34] In order to circumvent the moisture sensitivity problem of Lewis acid, an excessive amount of $GaCl_3$ was added to achieve complete solubility. In preparing the solutions for ^1H NMR characterization, the concentration of the polymer nitromethane solutions was kept at 1.5 wt % in which $GaCl_3$:CH=N molar ratio was 1.5:1 and the concentration of $GaCl_3$ in the solution varied from 2.1 to 3.4 wt %.

Thin films of the polymers were spin coated onto optically flat fused silica substrate (5 cm in diameter) by using 1.5 wt % polymer in $GaCl_3$/nitromethane solutions in which the $GaCl_3$:CH=N molar ratio was 2:1. The typical condition for spin coating was 2500 rpm for 30 s and resulted in a film thickness of about 0.1 μm. Decomplexation of the $GaCl_3$/polymer complex films to obtain thin films of the pure polymers was done by immersing the films of the complexes in methanol for 1–2 days. Film quality, as judged by negligible scattering and well-defined transition in the optical absorption spectrum, was good except for thin films of P3MOPI, P4MOPI, PSMOPI, and 1,5-PMONI. These four polymers tended to form highly crystalline phases with $GaCl_3$, presumably due to the existence of polar methoxy side chains, and consequently the spin-coated thin films were opaque. In these four cases, the polymer thin films were alternatively spin coated from their DPP/formic acid solutions. Formic acid has a much lower boiling point and surface tension than *m*-cresol. Therefore, good adhesion between thin film and silica substrate could be obtained by using formic acid instead of *m*-cresol as the solvent. The polymer concentration used for spin coating was 3 wt % in formic acid in which DPP:CH=N molar ratio was 0.5:1. The typical condition was 2300 rpm for 30 s and resulted in a film thickness of about 0.2 μm. Decomplexation of the DPP/polymer films was achieved by immersing the films of complexes in triethylamine/ethanol overnight to afford thin films of the pure polymers.[10,35,36]

Instrumental Characterization. Thermogravimetric analysis (TGA) and differential scanning calorimetry (DSC) were done by using a DuPont Thermal Analysis Model 2100 based on an IBM PS/2 Model 60 computer and equipped with a Model 951 TGA and a Model 910 DSC units. TGA data were obtained in flowing nitrogen at a heating rate of 10 °C/min. DSC thermograms were obtained in nitrogen at a heating rate of 20 °C/min. Optical absorption spectra were taken on a Perkin-Elmer Lambda 9 UV–vis–near IR spectrophotometer.

Fourier transform infrared (FTIR) spectra were taken at room temperature by using a Nicolet Model 20 SXC spectrometer under nitrogen purge. Samples were in the form of KBr pellets or films coated on NaCl disks. For example, the FTIR spectrum of pure PBHOPI was obtained by using a KBr pellet whereas the spectrum of PBHOPI/$GaCl_3$ complex was obtained from a film cast on NaCl disk. The ^1H NMR spectra were taken at 300 MHz by using a General Electric QE 300 instrument. The solutions for NMR spectra were prepared by dissolving the polymers in deuterated nitromethane (CD_3NO_2) containing $GaCl_3$.

The electrochemical equipment used for cyclic voltammetry experiments was an EG&G Princeton Applied Research Potentiostat/Galvanostat Model 270 with option board 96.[31] Data were collected and analyzed using Electrochemical Analysis System Software for Model 270 on a IBM PS/2 computer. In all experiments, acetonitrile (99.5+%, Aldrich) was used as the solvent to prepare the 0.1 M tetrabutylammonium tetrafluoroborate (TBATFB) (99+%, Fluka) electrolyte solution. Platinum wire electrodes were used as both the counter and working electrodes, and silver/silver ion (Ag in 0.1 M $AgNO_3$ in the electrolyte solution, Bioanalytical System) was used as the reference electrode. The potential values referenced to Ag/Ag^+ electrode were checked by reference to an internal standard, ferrocenium/ferrocene (Fc^+/Fc). A 3 wt % solution of the polymer in DPP/*m*-cresol or $GaCl_3$/nitromethane was used to prepare the polymer film on Pt electrode. The thin films of pure polymers were obtained by the regeneration procedures described previously. The cyclic voltammograms were obtained at a voltage scan rate of 20 mV/s. The potential values obtained versus Fc^+/Fc standard were converted to the saturated calomel electrode (SCE) scale by adding a constant of 0.1588 V to them.[37-39]

Scheme 1

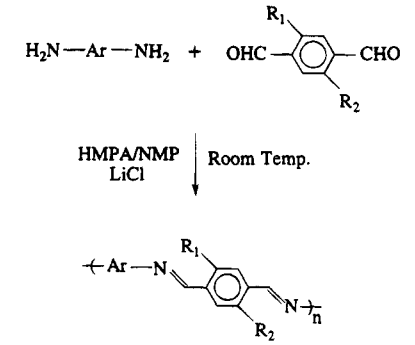

Results and Discussion

Polymer Synthesis and Intrinsic Viscosity. The series of new conjugated aromatic polyimines in Chart 1 were prepared by the solution polymerization of aromatic diamines with aromatic dialdehydes using the general reaction scheme depicted in Scheme 1 which is similar to the literature approach.[16] The polymerization reaction yield was high for nine of the polymers, with yields of 91–96%. Six had yields of 83–88% and five had yields of 43–76%. The polymers from 2,5-dichloro-1,4-phenylenediamine, Cl_2-PPI (**3a**) and Cl_2-PMOPI (**3b**), had the poorest polymerization yields with 43 and 60%, respectively. Of the aromatic dialdehydes polymerized with various aromatic diamines, 2,5-dihydroxyterephthalaldehyde gave the lowest yields 72–86%. The poor yield of some of the polymerizations is an indication of the poor reactivity of some of the co-monomers and the premature precipitation of some of the polymers due to poor solubility in the HMPA/NMP reaction medium.

The intrinsic viscosity [η] of the 20 conjugated aromatic polyimines at 30 °C in $GaCl_3$/nitromethane, in which the $GaCl_3$:CH=N molar ratio was 2:1, are shown in Table 1. The conjugated aromatic polyimines are also soluble in strong protonic acid such as sulfuric acid and methanesulfonic acid. Previously reported viscosity data on aromatic polyimines were obtained in acid media[14,16] and a Mark–Houwink equation was reported for poly(2-methyl-1,4-phenylenemethylidynenitrilo-1,4-phenylenenitrilomethylidyne) (PMPI, **1d** in Chart 1) in sulfuric acid.[40] However, acid-catalyzed hydrolysis of the polymers in strong protonic acid may lead to significant degradation and thus the true molecular weight cannot be obtained in such solvents.[10,16,17] In regard to this limitation, the advantage of using nitromethane–$GaCl_3$ as a solvent for viscosity measurement is obvious.

The intrinsic viscosity values listed in Table 1 vary from 0.47 dL/g for 1,5-PMONI (**8b**) to 2.29 dL/g for PTHOPI (**6c**). On the basis of the comparisons of

Table 1. Intrinsic Viscosity [η] in $GaCl_3$/Nitromethane at 30 ± 0.1 °C, Thermal Decomposition Temperature (T_D) and Melting Temperature (T_m) under Nitrogen Purge of Conjugated Aromatic Polyimines

polymer	[η], dL/g	T_D, °C	T_m, °C
2a MO-PPI	1.17	394	–[a]
2b P3MOPI	1.23	372	317
2c MO-PHOPI	0.77	369	–
3a Cl_2-PPI	0.77	445	–
3b Cl_2-PMOPI	1.14	413	–
4a PBPI	1.74	527	434, 454
4b PBMOPI	1.70	398	–
4c PBHOPI	1.73	444	–
5a MO-PBPI	2.22	409	–
5b P4MOBPI	2.27	386	311
5c MO-PBHOPI	2.08	356	–
6a PTPI	2.08	526	405, 450
6b PTMOPI	2.27	399	–
6c PTHOPI	2.29	449	–
7a PSPI	0.87	508	432
7b PSMOPI	0.91	391	322
7c PSHOPI	1.08	416	–
8a 1,5-PNI	0.67	453	–
8b 1,5-PMONI	0.47	403	–
8c 1,5-PHONI	0.62	395	–

[a] No melting transition was observed.

polymers with different backbone structures, the intrinsic viscosity values reflect in part the polymer chain rigidity. For example, three members of the *p*-biphenylene-linked polyimines **4**, i.e. PBPI, PBMOPI, and PBHOPI, consistently have higher intrinsic viscosity than their stilbene-linked counterparts (PSPI, PSMOPI, and PSHOPI). The intrinsic viscosities of the *p*-terphenylene polymers (**6a**–**6c**) are also relatively large (2.08–2.29 dL/g) because of the greater chain stiffness of these polyimines due to the rodlike nature of *p*-terphenylene. The low intrinsic viscosity (0.47–0.67 dL/g) as well as the relatively low polymerization yield (72–83%) of the 1,5-naphthalene-linked polyimines are due to the low reactivity of 1,5-diaminonaphthalene and the crackshaft topology the 1,5-naphthalene introduces into the polymer chain.

The molecular weight of the aromatic polyimines whose intrinsic viscosity is given in Table 1 is clearly subjected to the limitation of the reaction scheme employed since the polymers generally precipitated out of the polymerization media. However, the good film-forming ability of all of the 20 polymers indicates that their molecular weights are reasonably high. If necessary and depending on the intended applications, the molecular weight of these polyimines could be increased by using Morgan's two-step synthetic scheme involving solution polymerization and subsequently melt polymerization reaction.[16] Using such a two-step polymerization process Morgan et al.[16] obtained an inherent viscosity of 6 dL/g for a 0.5 wt % solution of PMPI (**1d**) in concentrated sulfuric acid. We have measured a melting temperature of about 250 °C and an onset of decomposition of about 420 °C in nitrogen for PMPI,[10] indicating that further melt polymerization is feasible. Incorporation of bulky side groups is another method that could be used to increase the molecular weight of aromatic polyimines. Reinhardt and Unroe have reported an intrinsic viscosity of 1.75 dL/g for oxydecyl-substituted aromatic polyimines in sulfuric acid.[18]

Soluble Complexes in Organic Solvents and Thin Film Processing. The solubilization of all the aromatic polyimines in Chart 1 in organic solvents such as nitromethane and nitrobenzene was achieved by coordination complexation of the polymers by Lewis acids such as $GaCl_3$ and $AlCl_3$. The success of Lewis acid complexation and solubilization of aromatic polyimines and many other classes of heterochain polymers in organic solvents demonstrates the versatility of the approach.[10,30–34] This solubilization of the aromatic polyimines in organic solvents has facilitated the detailed characterization of their molecular structures by ^1H NMR spectroscopy as well as the preparation of their thin films and coatings for investigation of the solid state properties of interest in electronic, optoelectronic, and photonic applications.[7,9]

Except the dihydroxy-substituted derivatives, the aromatic polyimines in Chart 1 also form soluble diphenyl phosphate (DPP) or di-*m*-cresyl phosphate (DCP) complexes in *m*-cresol or formic acid. The complexation

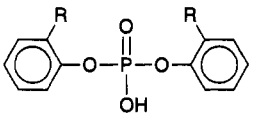

R = H (DPP)
R = CH_3 (DCP)

involves protonation of imine nitrogen on the polymer chain. However, caution needs to be taken in using formic acid as a solvent because formic acid itself can compete with DPP or DCP in protonating the polymer. Formic acid is a good substitute for *m*-cresol to prepare thin films of polyimines by spin coating because it is relatively more volatile and exhibits good adhesion to silica substrate. However, for the purpose of studying the optical absorption spectra of the complexes, the polymer/DPP complexes were prepared from solutions in *m*-cresol to avoid any possible inhomogeneous complexation of the polymers by DPP and formic acid.

The reversibility of Lewis acid or diaryl phosphate complexation by using methanol or triethylamine/ethanol as regeneration solvent, respectively, has been demonstrated by TGA and FTIR spectroscopic analysis of a series of other conjugated aromatic polyimines.[10] By using the same characterization procedures, the regenerated and the pristine polymers were shown to be identical prior to the study of their molecular structures and investigation of the electroactive and photoactive properties presented in subsequent sections.

Characterization of Molecular Structure. The ^1H NMR spectra of all the aromatic polyimines in Chart 1 were obtained in deuterated nitromethane containing $GaCl_3$. Typical ^1H NMR spectra of the aromatic polyimines are exemplified by those of PBPI and PTPI which are shown in Figures 1 and 2, respectively. The assignment of the chemical shifts of all resonances in the NMR spectra are listed in Table 2. The two ^1H NMR spectra in Figures 1 and 2 have resonance peaks that can readily be assigned to the phenylene and imine protons of PBPI and PTPI. The resonance of the phenylene protons occurs at 8.20 and 8.65 ppm in PBPI, and at 8.00, 8.15, and 8.60 ppm in PTPI. The 9.80 and 9.70 ppm resonances in Figures 1 and 2 are assigned to the imine protons of PBPI and PTPI, respectively. The chemical shift and the integration of resonances are in good agreement with the proposed polymer structures.

Table 2 also shows all of the chemical shifts of the ^1H NMR spectra of all the aromatic polyimines in Chart 1. The chemical shifts of the imine and phenylene proton resonances are generally in the range of 9.40–9.85 ppm and 7.75–8.80 ppm, respectively, depending on the polymer structure (Table 2). Compared to the reported

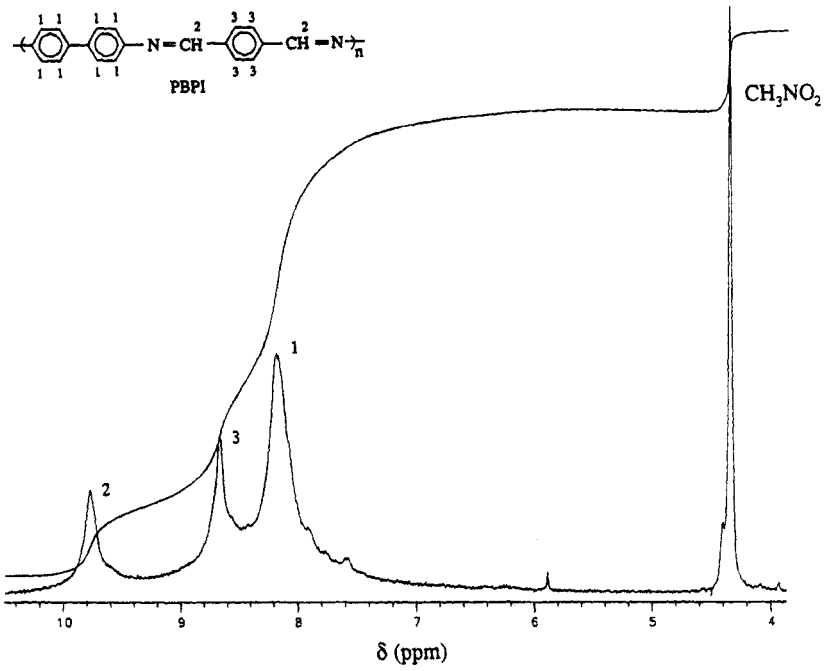

Figure 1. ^1H NMR spectrum of PBPI in $CD_3NO_2/GaCl_3$.

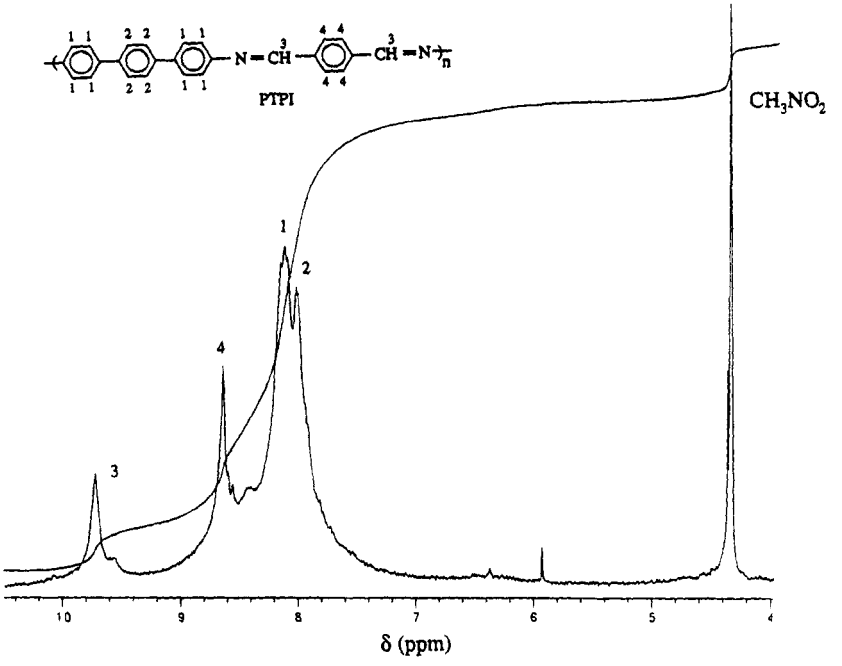

Figure 2. ^1H NMR spectrum of PTPI in $CD_3NO_2/GaCl_3$.

^1H NMR spectra (in $CDCl_3$) of soluble aromatic polyimines with long alkoxy side chains,[19] the imine and phenylene proton resonances of the aromatic polyimines in $CD_3NO_2/GaCl_3$ are shifted downfield because of the electron-deshielding effect of $GaCl_3$ complexation at the imine nitrogen sites.

A slight complication of the ^1H NMR spectra of some of the methoxy-containing polymers was observed in MO-PPI, P3MOPI, MO-PHOPI, and MO-PBHOPI due to the partial overlap of the methoxy proton resonances of the polymers with that of the methyl proton resonances (~4.35 ppm) of the nitromethane solvent (Table 2). A typical ^1H NMR spectrum of P3MOPI is shown in Figure 3 which indicates the overlap of the resonances of the methoxy protons on the different phenylene rings (~4.40 ppm) with the methyl protons in nitromethane (~4.35 ppm). However, given the correct correspondence of the other resonance peaks (phenylene and imine protons) and the same polymerization reaction as other methoxy-substituted polymers (e.g. PBMOPI) which show the correct integration for the methoxy protons, the structures of these four polymers are confirmed by comparisons of their ^1H NMR spectra with the other polyimines. Furthermore, FTIR spectroscopic characterization to be presented below provides additional evidence for the methoxy groups in these four polymers. Thus, overall the solution ^1H NMR spectra are in excellent agreement with the proposed structures.

FTIR spectra of all the aromatic polyimines in Chart 1 were obtained to confirm features of the proposed structures. We have previously reported the FTIR spectra of the four polyimines **1a–d** (Chart 1). The assignment of the characteristic vibrational bands in the

Table 2. Assignment of Chemical Shift of ^1H NMR Spectra in $CD_3NO_2/GaCl_3$

	chemical shift (ppm) of protons on functional groups				
polymer	phenylene	imine	methoxyl	hydroxyl	vinylene
2a MO-PPI	8.40, 8.65	9.85	4.40[a]		
2b P3MOPI	7.80, 8.15	9.60	4.40,[a] 4.50		
2c MO-PHOPI	7.80, 8.30	9.50	4.40[a]	6.10	
3a Cl_2-PPI	8.40, 8.80	9.85			
3b Cl_2-PMOPI	8.25, 8.60	9.75	4.60		
4a PBPI	8.20, 8.65	9.80			
4b PBMOPI	8.10, 8.20	9.50	4.50		
4c PBHOPI	8.05, 8.45	9.50		6.20	
5a MO-PBPI	7.75, 8.60	9.80	4.45		
5b P4MOPI	7.80, 8.10	9.50	4.45, 4.55		
5c MO-PBHOPI	7.75, 8.45	9.50	4.40[a]	6.00	
6a PTPI	8.00, 8.15, 8.60	9.70			
6b PTMOPI	8.00	9.45	4.45		
6c PTHOPI	7.90	9.40		5.85	
7a PSPI	8.00, 8.45	9.65			6.30
7b PSMOPI	8.00, 8.50	9.40	4.50		6.05
7c PSHOPI	7.80, 8.00	9.40		6.10	6.30
8a 1,5-PNI	8.10, 8.35, 8.60 8.80	9.90			
8b 1,5-PMONI	8.20, 8.30, 8.40 8.55	9.70	4.60		
8c 1,5-PHONI	8.05, 8.15, 8.40 8.50	9.60		5.95	

[a] Methoxyl protons overlapped with methyl protons in nitromethane.

FTIR spectra of the remaining 20 aromatic polyimines (**2a**–**8c**) in Chart 1 is summarized in Table 3. The most intense absorption band in the FTIR spectra of the aromatic polyimines is near 1600 cm^{-1} and it is assigned to the C=N stretching vibration. A second major structural feature of these polymers that is revealed by FTIR spectra is the substitution patterns of the *p*-phenylene rings. The FTIR spectra of all the polymers exhibit intense absorption bands in the 800–870 cm^{-1} region, except the 1,5-naphthalene-linked polymers which have intense vibrational bands in the 780–830 cm^{-1} region. These vibrational bands near 800–870 cm^{-1} are assigned to the out-of-plane C–H bending vibrations of the respective rings. This out-of-plane C–H bending together with the vibrational modes of the methoxy and hydroxy groups provide information about the methoxy, dimethoxy, and dihydroxy substitutions on some of the aromatic polyimines. For example, the out-of-plane C–H bending vibration of the unsubstituted PBPI absorbs energy at 840 cm^{-1}, whereas the dimethoxy-substituted PBMOPI absorbs at the lower energy of 825 cm^{-1} as a result of the 1,2,4-trisubstituted and 1,2,4,5-tetrasubstituted phenylene rings in PBMOPI compared to only 1,4-disubstituted phenylene rings in PBPI. Further evidence of the presence of the methoxy groups in the methoxy-substituted polymers comes from the appearance of the methyl C–H stretching vibration around 2930 cm^{-1} and the C–O–C stretching band near 1210–1260 cm^{-1} (Table 3).

FTIR spectroscopy also provides a facile method of elucidating the effects of intramolecular hydrogen bonding and Lewis acid or diaryl phosphate complexation on the molecular structures of the aromatic polyimines.[10,29] As stated previously, the dihydroxy-substituted aromatic polyimines (**1c**, **4c**, **5c**, **6c**, **7c**, and **8c**, Chart 1) are not soluble in DPP/*m*-cresol which indicates an inability to protonate the imine nitrogen by DPP. This observation suggests the existence of intramolecular hydrogen bonding in these materials and this can be confirmed by comparing the FTIR spectra of the pure polymers which are presumably hydrogen bonded intramolecularly and their $GaCl_3$ complexes. Since one of the objectives of obtaining the FTIR spectra of the dihydroxy-substituted polymers and their $GaCl_3$ complexes is to observe the O–H stretching vibration and the hydrogen bonding in the pristine polymers, extra care was taken to avoid moisture in the samples. This was done by storing the samples overnight in a vacuum oven at 100 °C prior to the experiments. A typical example of the FTIR spectra of the pure polymer and its $GaCl_3$ complex is shown in Figure 4 for PBHOPI and PBHOPI/$GaCl_3$. The corresponding assignments of vibrational modes are listed in Table 3 (**4c**). The absorption of O–H stretch in PBHOPI occurs at 3360 cm^{-1} and is of weak intensity. In contrast, the O–H stretch in PBHOPI/$GaCl_3$ is much more intense and is shifted to higher energy at 3480 cm^{-1}. This observation indicates that the O–H in pure PBHOPI is hydrogen-bonded, whereas that in the PBHOPI/$GaCl_3$ complex is free (Scheme 2). Similar features of O–H stretching vibration were also observed in the FTIR spectra of the other dihydroxy-substituted polyimines, such as MO-PHOPI, MO-PBHOPI, PTHOPI, PSHOPI, and 1,5-PHONI, and their $GaCl_3$ complexes. Another interesting comparison of the FTIR spectra of pure PBHOPI and PBHOPI/$GaCl_3$ complex is the shift of the C=N stretch. In the PBHOPI/$GaCl_3$ complex, the C=N stretching band is shifted to a higher frequency, 1640 cm^{-1}, compared to 1610 cm^{-1} in PBHOPI (Table 3). This shift to higher energy of the C=N stretching band on Lewis acid complexation is different from that observed in Lewis acid complexes of nonconjugated polymers such as aliphatic polyamides, in which the characteristic vibrational band of C=O is shifted to a lower frequency on Lewis acid coordination to the carbonyl oxygen.[30] However, FTIR spectroscopic studies of the Lewis acid complexes of many other classes of conjugated polymers show that coordination to groups such as C=N results in shift of the vibrational absorption frequency to higher values as observed here for the $GaCl_3$ complexes of aromatic polyimines. This shift of C=N stretching band to high absorption frequency in the $GaCl_3$ complexes can be rationalized by a redistribution of electron density from the π-electron system of the conjugated polymer. This also means that significant changes in the electronic absorption spectra can be expected on complexation.

The FTIR spectra of the DPP complexes of the polymers were similarly obtained to characterize the molecular structures of the polyimine/DPP complexes and to elucidate the interactions between imine nitrogen and DPP. Details of such spectra of the polymer complexes with DCP were described in our previous study.[29] Evidence for the protonation of the imine nitrogens by DPP includes the occurrence of a broad absorption at ~2615 cm^{-1} which can be assigned to N^+–H stretch.[29] A shift to higher frequency of the C=N stretch ($\Delta\nu \sim 60$ cm^{-1}) is also observed in DPP complexes as in the case of $GaCl_3$ complexes. This increased frequency of C=N stretching vibration with complexation can be attributed to the coupling between C=N stretching and C=N–H bending motion,[41] or a rehybridization effect which leads to electron density redistribution in the C=N linkage.[42]

Additional characterization of the molecular structure of the polymers was done by elemental analysis. Because all the polymers in this study were prepared by the same polymerization reaction conditions and since their structures are very similar, only three selected

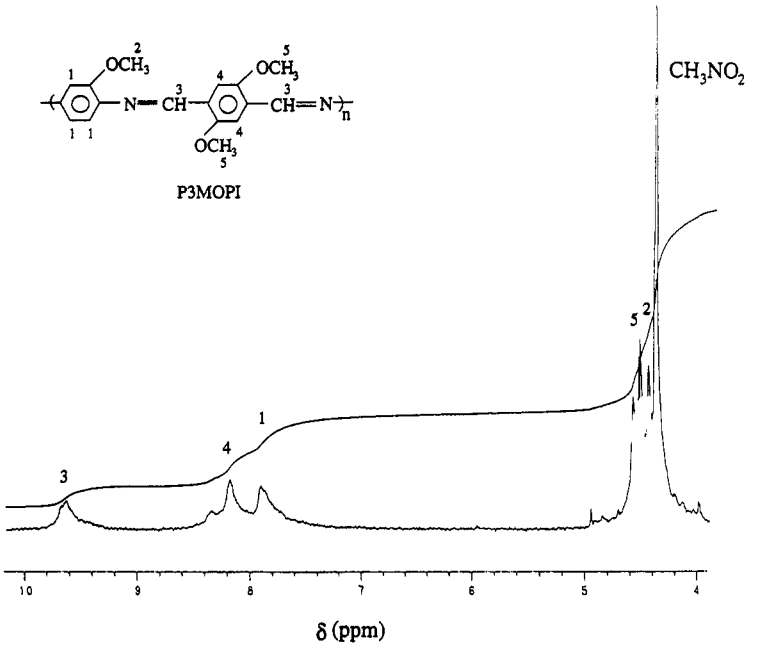

Figure 3. ^1H NMR spectrum of P3MOPI in $CD_3NO_2/GaCl_3$.

Table 3. Assignment of FTIR Spectra of Conjugated Aromatic Polyimines

polymer	C=N stretch	out-of-plane C–H bend	methyl C–H stretch	C–O–C stretch	O–H stretch	C–C ring stretch	C=C asymmetric stretch
2a MO-PPI	1615(s)	835(s)	2935(w)	1260(m)		1490(m)	
2b P3MOPI	1610(s)	830(s)	2940(w)	1210(m)		1485(m)	
2c MO-PHOPI	1600(s)	800–870(s)	2925(w)	1260(m)	3370(w)	1490(m)	
3a Cl_2-PPI	1610(s)	835(s)				1490(m)	
3b Cl_2-PMOPI	1610(s)	830(s)	2930(w)	1230(m)		1490(m)	
4a PBPI	1620(s)	840(s)				1485(m)	
4b PBMOPI	1615(s)	825(s)	2930(w)	1210(m)		1485(m)	
4c PBHOPI	1610(s)	825–880(s)			3360(w)	1490(m)	
PBHOPI/$GaCl_3$	1640(s)	825–880(s)			3480(s)	1490(m)	
5a MO-PBPI	1620(s)	815(s)	2935(w)	1240(m)		1485(m)	
5b P4MOBPI	1615(s)	810(s)	2930(w)	1240(m)		1485(m)	
5c MO-PBHOPI	1610(s)	805–865(s)	2935(w)	1245(m)	3350(w)	1485(m)	
6a PTPI	1605(s)	815(s)				1485(m)	
6b PTMOPI	1615(s)	815(s)	2930(w)	1210(m)		1485(m)	
6c PTHOPI	1615(s)	815(s)			3400(w)	1485(m)	
7a PSPI	1620(s)	845(s)				1500(m)	1605(m)
7b PSMOPI	1615(s)	835(s)	2935(w)	1210(m)		1485(m)	1590(m)
7c PSHOPI	1610(s)	835(s)			3375(w)	1495(m)	1585(m)
8a 1,5-PNI	1620(s)	785(s)				1500(m)	
8b 1,5-PMONI	1610(s)	785(s)	2935(w)	1215(m)		1490(m)	
8c 1,5-PHONI	1600(s)	780(s)			3370(w)	1500(m)	

polymers were characterized by elemental analysis. The results of the elemental analyses of MO-PHOPI, MO-PBHOPI, and PSPI are collected in the Experimental Section. Compared to the calculated content of nitrogen, hydrogen, and oxygen in the proposed structures, the elemental analyses show excellent agreement. However, a deficiency in carbon content of 1.7–2.9% was observed and this is likely a result of the difficulties in burning these high-temperature polymers.

Thermal Stability and Morphology. Figures 5 and 6 show the TGA and DSC thermograms, respectively, of conjugated aromatic polyimines with various backbone structures, PBPI (curve a), PTPI (curve b), PSPI (curve c), and 1,5-PNI (curve d). TGA was done at a heating rate of 10 °C/min and DSC was done at a heating rate of 20 °C/min, and both were under flowing nitrogen. The thermal decomposition temperature (T_D) and melting temperature (T_m) of the polymers are collected in Table 1. The onset of thermal decomposition of PBPI, PTPI, and PSPI under flowing N_2 is 527, 526, and 509 °C, respectively. Compared to the previously reported PPI (**1a**) (T_D = 504 °C),[10] incorporation of more phenylene rings in the polymer backbone results in an increase of thermal stability, whereas the thermal stability is only slightly higher in PSPI where a stilbene replaces a *p*-pheylene linkage. Introduction of a fused naphthalene ring structure into the aromatic polyimine backbone as in 1,5-PNI reduces thermal stability and the resulting decomposition temperature is decreased about 50 °C compared to PPI. As each of the main backbone polymer is substituted with side groups, the thermal stability is reduced significantly. This is exemplified by comparing the onset of thermal decomposition of MO-PPI (T_D = 394 °C), PMOPI (T_D = 386 °C), and P3MOPI (T_D = 372 °C) (Table 1) with that of PPI (T_D = 504 °C).[10]

In Figure 6, the observed multiple endothermic transitions in the DSC thermograms of PBPI (434 and 454 °C) and PTPI (405 and 450 °C) are probably due to a distribution of crystalline size or degree of crystalline perfection in these materials. It is also shown in Figure 6 that PSPI exhibits a melting transition peak at 432 °C. All these three polymers have a higher melting temperature compared to the parent aromatic polyimine

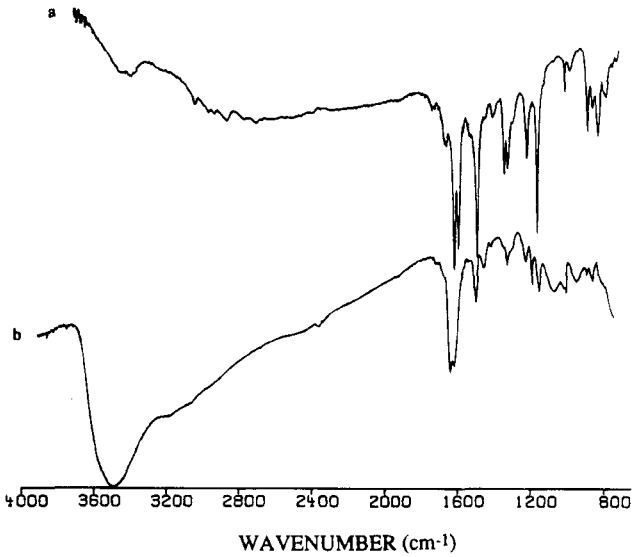

Figure 4. FTIR spectra of KBr pellet of PBHOPI (a) and of thin film on NaCl plate of PBHOPI/$GaCl_3$ (b).

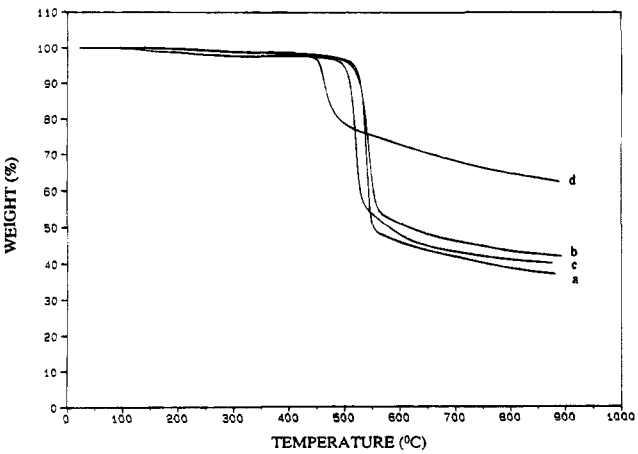

Figure 5. Thermogravimetric analysis (TGA) thermograms of PBPI (a), PTPI (b), PSPI (c), and 1,5-PNI (d).

Scheme 2

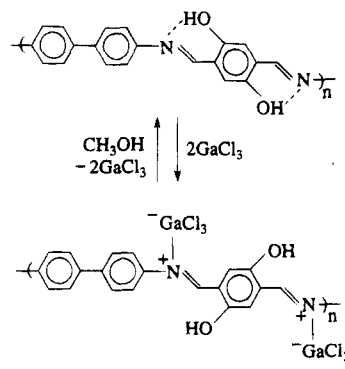

PPI (T_m = 385 °C).[10] The naphthalene-linked polymer, 1,5-PNI, does not exhibit any phase transition up to ~400 °C (Figure 6, curve d). A significant decrease of the melting temperature was expected in the side-group-substituted polymers. However, the melting transition may not be observable prior to decomposition because of the concomitant decrease of thermal stability due to side-group substitution. Therefore, only P4MOBPI, P3MOPI, and PSMOPI exhibit observable melting transition at 311, 317, and 322 °C, respectively (Table 1).

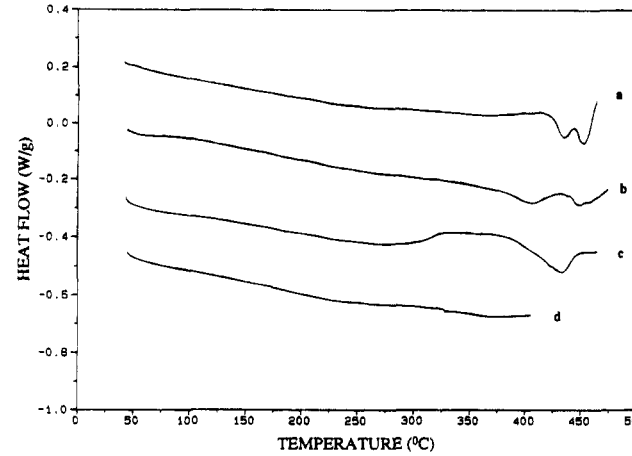

Figure 6. Differential scanning calorimetry (DSC) thermograms of PBPI (a), PTPI (b), PSPI (c), and 1,5-PNI (d).

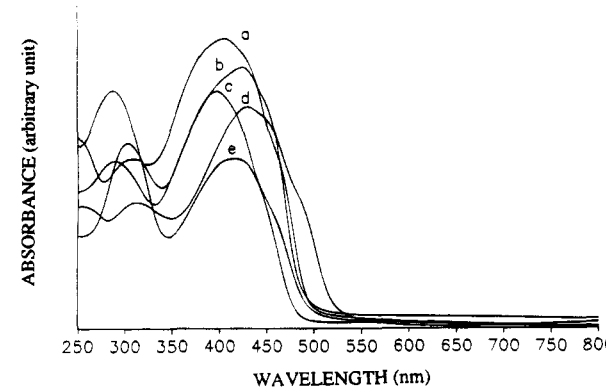

Figure 7. Optical absorption spectra of thin films of PPI (a), PBPI (b), PTPI (c), PSPI (d), and 1,5-PNI (e).

Optical Absorption Spectra of Thin Films of Polymers and Complexes. Optical-quality thin films of the $GaCl_3$ or DPP complexes of the aromatic polyimines and the subsequently regenerated pure polymers were prepared to investigate the effects of structure on optical absorption and the related electronic structures and properties of the materials. In the following discussion, the effects of structural modifications will be explored in terms of the effects of backbone variation and the effects of side-group substitution and of complexation.

Effects of Backbone Variation. The optical absorption spectra of thin films of PBPI (curve b), PTPI (curve c), PSPI (curve d), and 1,5-PNI (curve e) are shown in Figure 7. The previously reported optical absorption spectrum of PPI (curve a) is also included in Figure 7 for comparison.[10] The lowest energy absorption maximum λ_{max} and the optical absorption edge E_g are collected in Table 4. A comparison of the λ_{max} and E_g of PBPI to PPI shows that incorporation of a *p*-biphenylene linkage in the aromatic polyimines results in a 15-nm increase of λ_{max} compared to the phenylene-linked PPI (Table 4). However, the optical gap of PBPI (E_g = 2.53 eV) is essentially identical to PPI (E_g = 2.50 eV). The effect of incorporation of more phenylene rings on the polymer backbone is more obvious in PTPI, which exhibits a noticeable blue shift in the optical absorption spectrum (E_g = 2.58 eV, λ_{max} = 396 nm) compared to both PPI and PBPI (Table 4). It is interesting to note that the completely *p*-phenylene-linked conjugated polymer, poly(*p*-phenylene), was reported to exhibit a large π-π^* gap of 2.8 eV.[43] There is about a 25 nm increase of λ_{max} and a 0.12 eV reduction

Table 4. The Electronic Absorption Maxima (λ_{max}) and the Absorption Edge (E_g) of Conjugated Aromatic Polyimines

polymer	λ_{max}, nm (eV)	absorption edge E_g, nm (eV)
1a PPI	405 (3.06)	496 (2.50)
1b PMOPI	447 (2.77)	529 (2.34)
1c PHOPI	494 (2.51)	600 (2.07)
1d PMPI	406 (3.05)	497 (2.49)
2a MO-PPI	430 (2.88)	515 (2.41)
2b P3MOPI	460 (2.70)	555 (2.23)
2c MO-PHOPI	510 (2.43)	610 (2.03)
3a Cl_2-PPI	400 (3.10)	496 (2.50)
3b Cl_2-PMOPI	450 (2.76)	550 (2.25)
4a PBPI	420 (2.95)	490 (2.53)
4b PBMOPI	440 (2.82)	520 (2.38)
4c PBHOPI	485 (2.56)	570 (2.17)
5a MO-PBPI	410 (3.02)	505 (2.46)
5b P4MOBPI	450 (2.76)	540 (2.30)
5c MO-PBHOPI	490 (2.53)	605 (2.05)
6a PTPI	396 (3.13)	480 (2.58)
6b PTMOPI	428 (2.90)	502 (2.47)
6c PTHOPI	460 (2.70)	540 (2.30)
7a PSPI	430 (2.88)	520 (2.38)
7b PSMOPI	445 (2.79)	540 (2.30)
7c PSHOPI	500 (2.48)	590 (2.10)
8a 1,5-PNI	410 (3.02)	495 (2.51)
8b 1,5-PMONI	430 (2.88)	510 (2.43)
8c 1,5-PHONI	440 (2.82)	550 (2.25)

of optical gap when stilbene replaces one *p*-phenylene ring of PPI as shown in the optical absorption spectrum of PSPI compared to PPI. The λ_{max} and E_g values of 1,5-PNI are virtually the same as for PPI (Table 4). The observed changes of optical absorption spectra when the backbone structure is varied can be attributed to the modification of polymer chain planarity. Thus, the more coplanar vinylene relative to imine linkage leads to a decrease of E_g in PSPI, whereas the more nonplanar biphenylene and terphenylene linkages result in an increase of E_g in PBPI and PTPI.

The similarity of the optical absorption spectra as judged from the λ_{max} and E_g values of the 1,5-naphthalene-linked polymer 1,5-PNI, the *p*-phenylene-linked polymer PPI, and the *p*-biphenylene-linked PBPI is especially noteworthy in view of the prior speculations about the greater chain planarity of 1,5-PNI relative to the others. Wagener and co-workers[22] have reported the electrical conductivity of iodine-doped *pressed pellets* of several conjugated aromatic polyimines, including PPI, PBPI, and 1,5-PNI. They found that iodine-doped 1,5-PNI had about 2–3 orders of magnitude higher conductivity than PPI and PBPI. They explained their results in terms of the greater backbone planarity of 1,5-PNI compared to PPI, PBPI, and other conjugated aromatic polyimines.[22] Our optical absorption spectra on *thin films* of these conjugated aromatic polyimines clearly show that incorporation of the 1,5-naphthalene linkage into the backbone of this class of polymers *does not* result in a more coplanar backbone structure as previously thought.[22] Thus, the observation of orders of magnitude improvement of electrical conductivity of iodine-doped 1,5-PNI compared to other aromatic polyimines must find alternative explanations. The observed differences in electrical conductivity could be a result of differences in (a) morphology of the pressed pellets; (b) ionization potential and hence the intrinsic oxidative dopability of the material; and (c) different levels of charge transfer and iodine doping, since the exact amount of doping or elemental compositions of the doped materials were not known. We will later present evidence ruling out possible explanation b. Also, we will present below optical absorption spectra of dihydroxy derivatives as well as complexes of these conjugated aromatic polyimines which indicate that efficiency of π-electron delocalization is actually decreased by introduction of 1,5-naphthalene linkage in the aromatic polyimine backbone.

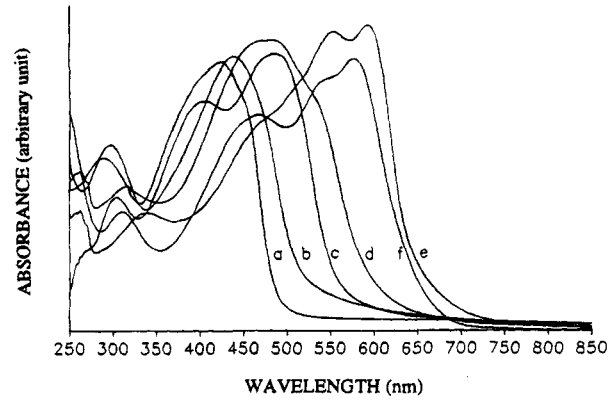

Figure 8. Optical absorption spectra of thin films of PBPI (a), PBMOPI (b), PBHOPI (c), PBPI/DPP (d), PBMOPI/DPP (e), and PBHOPI/$GaCl_3$ (f).

Effects of Side-Group Substitution and Complexation. Figure 8 shows the optical absorption spectra of thin films of polyimines **4a** (PBPI, curve a), **4b** (PBMOPI, curve b), and **4c** (PBHOPI, curve c) which exemplify the effects of dimethoxy and dihydroxy substitution on the *p*-phenylene ring of structure **4** (Chart 1). The lowest energy absorption maximum which is due to $\pi-\pi^*$ transition and the corresponding absorption edge (E_g) of the spectra in Figure 8 and of all the 24 conjugated aromatic polyimines in Chart 1 are collected in Table 4. PBMOPI with dimethoxy side groups has a 20 nm red shift in λ_{max} compared to the parent PBPI and a corresponding 0.15 eV reduction of E_g. As seen in Figure 8 and from Table 4, PBHOPI with dihydroxy side groups has an even greater red shift in λ_{max} and E_g of 65 nm and 0.36 eV, respectively, compared to PBPI. This striking feature of the optical absorption spectra of the side-group-substituted **4b** and **4c** compared to the parent **4a** is in fact a general feature of all the aromatic polyimines in Chart 1. The red shift of the λ_{max} of the dimethoxy-substituted polymers (**1b**, **2b**, **4b**, **5b**, **6b**, **7b**, **8b**) from their corresponding parent polymers (**1a**, **2a**, **3a**, **4a**, **5a**, **6a**, **7a**, **8a**) varied from 15 nm in PSMOPI (**7b**) to 40 nm in P4MOBPI (**5b**). The λ_{max} red shift of the dihydroxy-substituted polymers, on the other hand, varied from 30 nm in 1,5-PHONI (**8c**) to 89 nm in PHOPI (**1c**). Thus, in general, the dihydroxy-substituted polymers have $\pi-\pi^*$ transition energies that are smaller than those of the dimethoxy-substituted polymers which in turn have smaller $\pi-\pi^*$ transition energies than their corresponding unsubstituted parent polymers.

The observed red shift of the electronic absorption spectra of the dimethoxy-substituted polymers (**1b**, **2b**, **3b**, **4b**, **5b**, **6b**, **7b**, **8b**) compared to their parent polymers (**1a**, **2a**, **3a**, **4a**, **5a**, **6a**, **7a**, **8a**, **9a**) can be explained by the greater electron density of the former conjugated polymers as a result of the electron-donating ability of the methoxy group. The case of Cl_2-PPI (**3a**) and Cl_2-PMOPI (**3b**) is slightly more complicated because of the simultaneous presence of electron-withdrawing chloro and electron-donating methoxy side groups in Cl_2-PMOPI which may induce ground-state charge transfer between 2,5-dichloro-1,4-phenylene and 2,5-dimethoxy-1,4-phenylene rings. A comparison of

Cl_2-PPI (**3a**) to PPI (**1a**) indicates that there is no change in electronic absorption spectra (Table 4) which is understandable considering the rather weak electron-withdrawing ability of the chloro group. The small decrease in $\pi-\pi^*$ transition and absorption edge energies in going from PMOPI to Cl_2-PMOPI is an indication that ground-state charge transfer may have occurred.

The observation that the dihydroxy-substituted polymers (**1c**, **2c**, **4c**, **5c**, **6c**, **7c**, **8c**) have significantly greater π-electron delocalization than the corresponding parent polymers and dimethoxy-substituted polymers (see λ_{max} and E_g values, Table 4) must be reconciled with the fact that the hydroxy group is a poorer electron-donating group than the methoxy group. As previously shown from our FTIR spectra results (Table 3), all the dihydroxy-substituted aromatic polyimines exhibit *intramolecular hydrogen bonding which planarizes the polymer backbone and consequently improves π-electron delocalization*. Thus, it is through the planarization of the polymer backbone induced by intramolecular hydrogen bonding that dihydroxy side group substitution exerts its main influence on the electronic structure of the aromatic polyimines rather than through inductive effects. It has been well documented in the literature[44-47] that the imine linkage (CH=N) is not coplanar with the neighboring phenylene ring in Schiff base molecules such as substituted *trans-N*-benzylideneaniline:

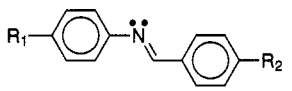

X-ray diffraction studies of *trans-N*-benzylideneaniline, a model compound of conjugated aromatic polyimine **1a**, have shown that the *N*-phenyl ring is twisted 55° from the CH=N plane.[44] Other literature reports have confirmed this nonplanar molecular structure of the aromatic Schiff base molecules and have shown that this is a result of the conjugation between the imine nitrogen lone pair electrons and the π-electrons on the *N*-phenyl ring.[45-47] This fundamentally noncoplanarity of the two rings linked by CH=N in Schiff base molecules also exists in the aromatic polyimines except where there is delibrate and effective intervention such as dihydroxy side-group substitution which induces intramolecular hydrogen bonding. Intramolecular hydrogen bonding prevents the nitrogen lone pair electrons from conjugation with adjacent ring π-electrons, thus leading to a coplanar polymer backbone structure and consequently more efficient π-electron delocalization.

This insight on the role of the imine nitrogen lone pair electrons on the planarity, and consequently the electronic structure, of the aromatic polyimines suggests that in addition to *intramolecular hydrogen bonding*, other strategies such as *complexation* or *quaternization* of the imine nitrogen should be effective for backbone planarization of this class of polymers. Effects of Lewis acid ($GaCl_3$) or diaryl phosphate (DPP) complexation of the imine nitrogens on the electronic structure of the aromatic polyimines were, therefore, explored through optical absorption spectroscopy. Figure 8 also shows the electronic absorption spectra of 1:1 DPP:CH=N complexes of PBPI (curve d) and PBMOPI (curve e) and 1:1 $GaCl_3$:CH=N complex of PBHOPI (curve f). The lowest energy $\pi-\pi^*$ absorption band parameters (λ_{max}, E_g) of these three complexes whose spectra are shown in Figure 8 as well as those of the DPP or $GaCl_3$ complexes of the other aromatic polyimines are collected in Table 5. A major feature of the absorption spectra of the complexes in Figure 8 is their dramatic red shift from those of the pristine polymers. The λ_{max} and E_g of the complexes are red shifted by 60–120 nm and 0.28–0.47 eV, respectively. Thus, either Lewis acid coordination complexation or protonic acid quarternization of the imine nitrogens of aromatic polyimines indeed induces backbone planarization with consequent more efficient π-electron delocalization compared to the pristine polyimines.

Table 5. The Optical Absorption Maxima (λ_{max}) and the Absorption Edge (E_g) of Thin Films of DPP and $GaCl_3$ Complexes of Conjugated Aromatic Polyimines

complex	λ_{max}, nm (eV)	absorption edge E_g, nm (eV)
PPI/DPP	490 (2.53)	577 (2.15)
PMOPI/DPP	560 (2.21)	670 (1.85)
PHOPI/$GaCl_3$	545 (2.28)	650 (1.91)
PMPI/DPP	496 (2.50)	586 (2.12)
MO-PPI/DPP	515 (2.41)	625 (1.98)
P3MOPI/DPP	560 (2.21)	690 (1.80)
MO-PHOPI/$GaCl_3$	585 (2.12)	720 (1.72)
Cl_2-PPI/DPP	420 (2.95)	584 (2.12)
Cl_2-PMOPI/DPP	531 (2.34)	676 (1.83)
PBPI/DPP	480 (2.58)	600 (2.07)
PBMOPI/DPP	590 (2.10)	650 (1.91)
PBHOPI/$GaCl_3$	580 (2.13)	655 (1.89)
MO-PBPI/DPP	490 (2.53)	610 (2.03)
P4MOBPI/DPP	630 (1.97)	700 (1.77)
MO-PBHOPI/$GaCl_3$	645 (1.92)	710 (1.75)
PTPI/DPP[a]		
PTMOPI/DPP	550 (2.25)	715 (1.73)
PTHOPI/$GaCl_3$	525 (2.36)	715 (1.73)
PSPI/DPP	520 (2.38)	670 (1.85)
PSMOPI/DPP	570 (2.18)	730 (1.70)
PSHOPI/$GaCl_3$	618 (2.01)	745 (1.66)
1,5-PNI/DPP[a]		
1,5-PMONI/DPP	500 (2.48)	580 (2.14)
1,5-PHONI/$GaCl_3$	535 (2.32)	640 (1.94)

[a] PTPI/DPP and 1,5-PNI/DPP are not stable.

A close examination of the electronic absorption spectra of the DPP or $GaCl_3$ complexes of all the new polyimines (Table 5) and comparison with the results of the pristine polymers (Table 4) reveals various effects of backbone planarity on electronic structure and the relative planarity of the aromatic polyimines. One interesting observation from the electronic spectra data of Tables 4 and 5 and Figure 8 is that all the DPP and $GaCl_3$ complexes have λ_{max} and E_g values that are red shifted compared to the dihydroxy-substituted polymers. This implies that the backbone planarity of the polyimine complexes is greater than that of the dihydroxy-substituted polymers; and hence that complexation induces a greater degree of molecular planarity than intramolecular hydrogen bonding. The intrinsic degree of molecular planarity of polymer repeat unit of the unsubstituted aromatic polyimines, based on the extent of π-electron delocalization measured by λ_{max} and E_g, is in the decreasing order: PSPI (**7a**) > PPI (**1a**) > PBPI (**4a**) > 1,5-PNI (**8a**) > PTPI (**6a**). This order of molecular planarity is only slightly modified by intramolecular hydrogen bonding as the dihydroxy-substituted polyimines have the following order of decreasing chain planarity: PSHOPI > PHOPI > PBHOPI > PTHOPI > 1,5-PNI. The least planar polymer chains are the *p*-terphenylene- and 1,5-naphthalene-linked polymers which can be rationalized in terms of the steric hindrances from the *ortho* hydrogens of *p*-terphenylene and the crackshaftlike topology of 1,5-naphthalene. The air stability of the DPP complexes of the polymers was found to be related to the intrinsic planarity of the pristine polyimines. Good environmental stability of

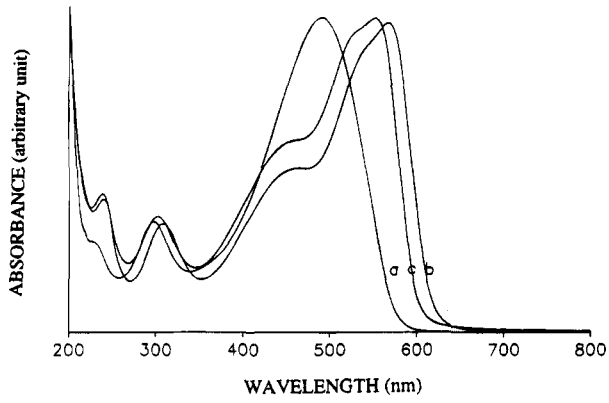

Figure 9. Solution optical absorption spectra of PBPI (a), PBMOPI (b), and PBHOPI (c) in sulfuric acid. Solution concentration $\sim 10^{-5}$ M of polymer repeat unit.

thin films of all the polyimine/DPP complexes was observed, as evidenced by identical appearance and optical absorption spectrum after a 6 month storage in air, except PTPI/DPP and 1,5-PNI/DPP complexes which were unstable in air. In the course of preparing films of the DPP complexes of PTPI and 1,5-PNI, red solutions of PTPI/DPP/*m*-cresol and 1,5-PNI/DPP/*m*-cresol were obtained compared to the yellow solutions of the pristine polymers in *m*-cresol. However, as *m*-cresol evaporated from cast films of DPP complexes of these two polymers, decomplexation occurred resulting in a color change from red to yellow. This indicated that the DPP complexes of PTPI and 1,5-PNI were only stable in solution unlike all the other aromatic polyimines whose DPP complexes were stable in both solution and the solid state. The relation of the stability of the DPP complex of a polymer to its molecular planarity is through the ability to stabilize the cations formed on the polymer chain by DPP complexation.

Another interesting effect of backbone planarity on electronic structure is revealed by comparing the increase of λ_{max}, as a result of the inductive effect of dimethoxy substitution, in the pure polymers and in the DPP complexes. For example, there is a 20 nm increase of λ_{max} in going from PBPI to PBMOPI, whereas a 110 nm increase of λ_{max} is observed in going from PBPI/DPP complex to the PBMOPI/DPP complex (Tables 4 and 5). This remarkably larger increase of λ_{max} due to electron-donating dimethoxy substitution in the polyimine/DPP complexes compared to the pure polymers, is also observed in all the dimethoxy-substituted polymers and their corresponding complexes (Tables 4 and 5). This observation indicates that the inductive effect of side-group substitution becomes more pronounced as the polymer backbone becomes more planar, in good agreement with experimental observations on a Schiff base molecule, *trans-N*-benzylideneaniline.[47]

Optical Absorption Spectra of Solutions. The solution optical absorption spectra of conjugated aromatic polyimines are exemplified by Figure 9 which shows the electronic absorption spectra of PBPI (**4a**) and its dimethoxy (**4b**) and dihydroxy (**4c**) derivatives in concentrated sulfuric acid. The corresponding absorption maximum $\lambda_{max}[\log \epsilon]$ values of the lowest energy $\pi-\pi^*$ transition in the solution optical absorption spectra of these three examples as well as all the other polyimines are listed in Table 6. A striking feature of these optical absorption spectra in sulfuric acid (Table 6) is their significant red shift compared to the solid state spectra of the same polymers (Table 4). For example, the λ_{max} of P4MOBPI in sulfuric acid is 617 nm compared to 430 nm in the solid state (Tables 4 and 6). The solution optical absorption spectra of other Schiff base polymers in acid media have been reported in the literature and were observed to exhibit similar features of red shift upon acid protonation.[10,17,48] The greater π-electron delocalization of the protonated conjugated aromatic polyimines in acid solution, as judged from λ_{max} (Tables 4 and 6), indicates that the polymer chains are relatively more planar in the protonated forms in solution than in the thin films of the pristine polymers. A comparison between the acid solution absorption spectra of the polymers (Table 6) and the thin film absorption spectra of the DPP or $GaCl_3$ complexes indicates that there is no systematic trend regarding which has the greater absorption maximum. Some of the complexes in the solid state have a larger λ_{max} and hence a more planar molecular structure (e.g. MO-PPI/DPP, PBMOPI/DPP, PBHOPI/$GaCl_3$, MO-PBHOPI/$GaCl_3$) than in acid solution, whereas some of the polymers (e.g. PBMOPI, PSMOPI, MO-PHOPI) have more extended electronic delocalization and hence improved molecular planarity in acid solution than in the solid complexes.

Table 6. The $\lambda_{max}[\log \epsilon]$ of the Lowest Energy $\pi-\pi^*$ Transition of the Solution Absorption Spectra in H_2SO_4

polymer	λ_{max}, nm (eV)	log ϵ
2a MO-PPI	495 (2.51)	4.08
2b P3MOPI	613 (2.02)	4.26
2c MO-PHOPI	602 (2.06)	4.23
3a Cl_2-PPI	420 (2.95)	4.02
3b Cl_2-PMOPI	591 (2.10)	4.13
4a PBPI	491 (2.53)	4.26
4b PBMOPI	566 (2.19)	4.38
4c PBHOPI	552 (2.25)	4.46
5a MO-PBPI	540 (2.30)	4.15
5b P4MOBPI	617 (2.01)	4.20
5c MO-PBHOPI	610 (2.03)	4.26
6a PTPI	524 (2.37)	4.08
6b PTMOPI	579 (2.14)	4.50
6c PTHOPI	547 (2.27)	4.24
7a PSPI	549 (2.26)	4.44
7b PSMOPI	600 (2.07)	4.53
7c PSHOPI	575 (2.16)	4.56
8a 1,5-PNI	446 (2.78)	3.88
8b 1,5-PMONI	522 (2.38)	4.00
8c 1,5-PHONI	515 (2.41)	4.02

The optical absorption spectra of the dimethoxy-substituted polymer (PBMOPI, curve b) and the corresponding dihydroxy derivative (PBHOPI, curve c) in sulfuric acid are very similar in line shape and are only slightly different in absorption maximum and long wavelength absorption edge (Figure 9). A similar observation was made between PMOPI and PHOPI in sulfuric acid.[10] An explanation of this observation is that hydrolysis reaction occurs in sulfuric acid which converts methoxy groups to hydroxy groups. An alternative explanation is that once the imine nitrogens are protonated in sulfuric acid, both the dihydroxy and the dimethoxy derivatives exhibit similar degrees of molecular planarity and the inductive effects of the hydroxy and the methoxy groups become relatively minor and results in similar contributions to electronic delocalization.

Electrochemical Properties and Electronic Structure. We have used cyclic voltammetry to investigate the reduction and oxidation (redox) potentials of the conjugated aromatic polyimines of Chart 1 in order to further understand their electronic structure and electrochemical properties and to assess their intrinsic potential as conducting polymers and optoelectronic

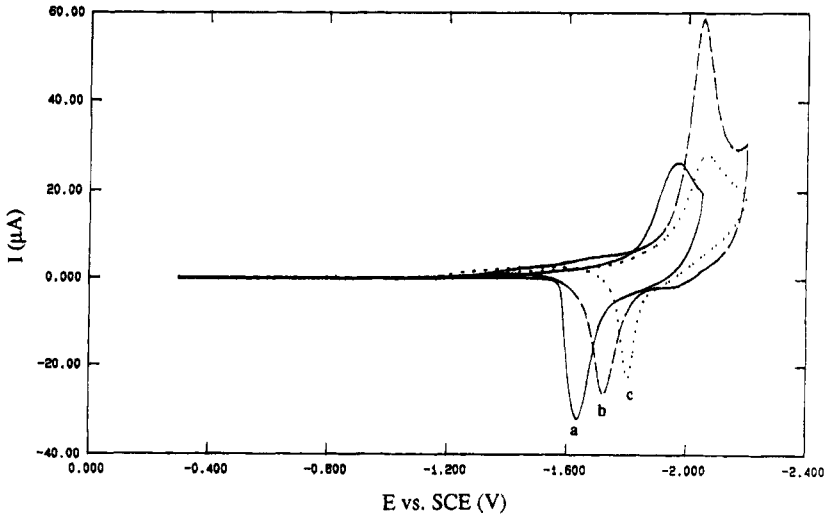

Figure 10. Cyclic voltammograms of the reduction of PPI (a), PBPI (b), and PTPI (c) in 0.1 M $TBABF_4$ in acetonitrile.

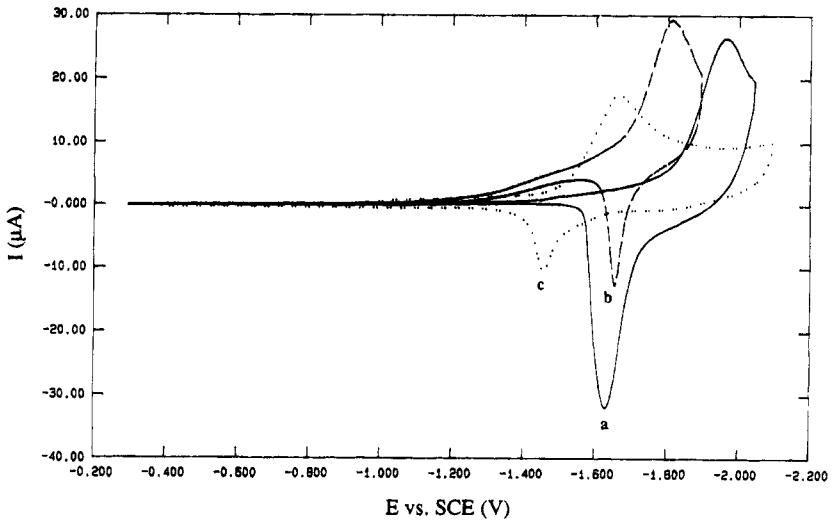

Figure 11. Cyclic voltammograms of the reduction of PPI (a), PMOPI (b), and Cl_2-PPI (c) in 0.1 M $TBABF_4$ in acetonitrile.

materials. There was a previous report on the cyclic voltammogram of an alkyl-substituted aromatic polyimine.[49] However, the polymer investigated gradually dissolved during repeated cyclic voltammetric scans and therefore clear redox potentials could not be assigned to the polymer.[49] The present study represents the first successful measurement of the electrochemical properties of conjugated aromatic polyimines and the electrochemical assessment of their ground state charge transfer characteristics or dopability to conducting polymers. This was facilitated by our ability to prepare high-quality thin films from soluble complexes of the polymers. In the following we present the measured redox potentials and explore the effects of backbone structure and side group substitution on the electrochemical properties and electronic structure.

Electrochemical Reduction. Figure 10 shows the cyclic voltammograms (CVs) of the reduction of the parent conjugated polyimine PPI (curve a), PBPI (curve b), and PTPI (curve c). It is seen in the figure that all three polyimines exhibit reversible one-electron reduction. A deep green color, as opposed to the yellow color in the neutral state, was observed during the reduction of PPI. The formal potential for reduction, ($E_0' = (E_{pa} + E_{pc})/2$), of PPI is −1.78 V (vs SCE). Changing the polymer backbone from PPI to PBPI and PTPI results in a decrease of the formal potential for reduction E_0' by 0.11 and 0.15 V to −1.89 and −1.93 V, respectively. Figure 11 shows the reduction CVs of representative side-group-substituted conjugated polyimines PMOPI (curve b) and Cl_2-PPI (curve c), compared to PPI (curve a). Similar to the parent PPI, PMOPI, and Cl_2-PPI exhibit stable one-electron reversible reduction waves. The reduction potential E_0' of PMOPI and Cl_2-PPI is −1.71 and −1.52 V, respectively, which represents a significant increase of 0.26 V in the dichloro derivative compared to PPI (−1.78V). A summary of the peak potentials (E_{pa}, E_{pc}), onset reduction potential E_{onset}, and formal potential E_0' for electrochemical reduction of a series of 14 conjugated aromatic polyimines is given in Table 7.

A comparison of the reduction CV results in Table 7 shows that there is a fairly wide variation in the electrochemical properties with polymer molecular structure (Chart 1). The formal reduction potential E_0' and onset reduction potential E_{onset} vary by 0.41 and 0.48 V, respectively, among the 14 aromatic polyimines. The most readily reduced polymer in the series is Cl_2-PPI (**3a**) with a reduction potential of −1.52 V (SCE) and this is followed by Cl_2-PMOPI (**3b**) with a reduction potential of −1.58 V. The most difficult to reduce polymer in the series, on the other hand, is PTPI with a reduction potential of −1.93 V. One also sees that the variation of reduction potential with backbone structure is relatively small compared to the variation with side group substitution. It is interesting that the

Table 7. Electrochemical Reduction and Oxidation Potentials of Conjugated Aromatic Polyimines

	reduction[a]					oxidation[a]			
polymer	E_{pc}	E_{pa}	E_0'	E_{onset}	y[b] %	E_{pa}	E_{pc}	E_0'	E_{onset}
1a PPI	−1.94	−1.62	−1.78	−1.80	38	1.23	*c*	*c*	0.72
1b PMOPI	−1.79	−1.63	−1.71	−1.65	27	1.01	*c*	*c*	0.64
1c PHOPI	−1.91	*d*	*d*	−1.66	13	0.98	*c*	*c*	0.60
2a MO-PPI	−1.86	−1.68	−1.77	−1.68	29	1.04	*c*	*c*	0.70
2b P3MOPI	−1.78	−1.65	−1.72	−1.67	22	0.96	*c*	*c*	0.57
2c MO-PHOPI	−1.86	*d*	*d*	−1.68	6	0.65	*c*	*c*	0.40
3a Cl_2-PPI	−1.62	−1.42	−1.52	−1.46	32	1.20	*c*	*c*	0.98
3b Cl_2-PMOPI	−1.69	−1.47	−1.58	−1.49	21	1.20	*c*	*c*	0.65
4a PBPI	−2.06	−1.71	−1.89	−1.94	71	1.20	*c*	*c*	0.79
4b PBMOPI	−1.94	−1.76	−1.85	−1.82	42	1.13	*c*	*c*	0.73
6a PTPI	−2.05	−1.80	−1.93	−1.91	77	1.26	*c*	*c*	0.86
6b PTMOPI	−1.94	−1.82	−1.88	−1.84	48	1.10	*c*	*c*	0.80
7a PSPI	−2.00	−1.71	−1.86	−1.85	86	1.02	*c*	*c*	0.66
8a 1,5-PNI	−2.05	−1.70	−1.88	−1.84	52	0.98	*c*	*c*	0.81

[a] All potential values are in volts versus SCE. E_{pa} = anodic peak potential; E_{pc} = cathodic peak potential; E_0' = formal potential = $(E_{pa} + E_{pc})/2$; E_{onset} = onset potential. [b] Mole % of counterion ($N^+(C_4H_9)_4$) per polymer repeat unit during reduction. [c] Oxidation is not reversible. [d] Reduction is not reversible.

only two polymers in the series with nonreversible electrochemical reduction are PHOPI (**1c**) and MO-PHOPI (**2c**), both which exhibit intramolecular hydrogen bonding. This suggests that the intramolecular hydrogen bonding in these polymers interfers with the electron transfer process and the stabilization of the resulting radical anion.

The reduction CV results of the conjugated aromatic polyimines (Chart 1) show that each polymer, except the dihydroxy-substituted derivatives, exhibits a reversible reduction in accord with the electron dificient nature of the imine-linked aromatic polymer repeat units. The order of increasing reduction potential E_0' in the series of the polymers (Table 7) also represents the order of increasing n-type dopability of the polymers into conducting materials as well as the relative thermodynamic stability of the n-type doped materials. Another factor that is important to preparing a conducting polymer from a conjugated polymer is the amount of charge transfer during the doping process. Also shown in Table 7 is the mole %, *y*, of the counterion $N^+(C_4H_9)_4$ per polymer repeat unit achieved in electrochemical reduction. This represents the amount of electron transfer to the polymer backbone by electrochemical reduction and was determined from the total charge transferred and the total mass of the polymer film on the electrode. The mass of the polymer film on Pt electrode was calculated from the mass of a solution of known concentration coated onto the electrode. The total charge generated during reduction was obtained from integration of the current vs time cyclic voltammogram. The amount of charge transfer, *y*, collected in Table 7, varies from 22% of an electron transferred to P3MOPI to 86% of an electron transferred to PSPI among the series of polyimines that exhibit stable electrochemical reduction. Only 6−13% of electronic charge was transferred to the dihydroxy-substituted polymers (MO-PHOPI, PHOPI) which are also irreversible with respect to reduction. In general, the polyimines without side groups (PPI, PBPI, PTPI, PSPI, 1,5-PNI) had the largest amount of charge transfer, 38−86% of an electron. On the other hand, the dichloro derivatives (Cl_2-PPI, Cl_2-PMOPI) which exhibit the highest reduction potentials have only 21−32% of an electron transferred. In principle, the conjugated aromatic polyimines are excellent candidates for n-type doping to conducting polymers.

Electrochemical Oxidation. Figures 12 and 13 show representative CVs of the electrochemical oxidation of the conjugated aromatic polyimines, exemplified by the same polymers whose reduction CVs are shown in Figures 10 and 11. The electrochemical oxidation of this class of polymers is clearly not reversible under the conditions of our experiments. This result can be explained by the electron-deficient molecular structure of the polyimines. Although the oxidation process is not reversible so that the amount of charge transfer could not be quantified, we see a dramatic increase in the anodic current corresponding to oxidation of PBPI (curve b) and PTPI (curve c) relative to PPI (curve a) in Figure 12. The yellow color of the neutral polymers was changed to deep red color during the oxidation of PBPI and PTPI. The anodic peak potential (E_{pa}) and onset potential (E_{onset}) for oxidation of the series of polymers investigated are summarized in Table 7.

One of the main features of the oxidation CVs of this class of polymers is that in spite of the irreversibility of the oxidation process the oxidation peak potential E_{pa} and onset potential E_{onset} vary by 0.61 and 0.58 V, respectively, with molecular structure. MO-PHOPI (**2c**) is thermodynamically the easiest to oxidize polymer with E_{pa} and E_{onset} of 0.65 and 0.40 V (SCE). Not surprisingly, Cl_2-PPI (**3a**) is the most difficult to oxidize with E_{onset} of 0.98 V and E_{pa} of 1.20 V. This is consistent with the electron-withdrawing nature of the dichloro substituents in Cl_2-PPI. Another major feature of the oxidation CVs of these polymers is that the amount of charge transfer is generally small except in PBPI, PTPI, PSPI, and 1,5-PNI which are without side groups, judging qualitatively from the size of the anodic peak current since the oxidation was not reversible. On the basis of equal mass of polymers on the electrodes, the anodic peak current during the oxidation of PBPI and PTPI was about a factor of 15 larger than that of PPI. Roughly, this means that there is a greater charge transfer in PBPI and PTPI than PPI and this can be explained by the greater ability to accomodate a positive charge and stabilize the radical cation the more phenylene rings in the backbone.

The electrochemical oxidation of the conjugated aromatic polyimines suggests that although p-type (oxidative) doping to conducting polymers is feasible, the p-type doped state or the radical cation of the materials is relatively unstable. Thus, with regard to electrically conducting polymers from the conjugated aromatic polyimines, n-type doping is more promising than p-type doping. The present CV results also explain why only relatively poor electrical conductivity ($\sim 10^{-6}$ to 10^{-2} S/cm) have been achieved to date in the reported studies of oxidatively (I_2) doped conjugated polyazomethines.[22]

Also, these CV results provide a possible explanation for why iodine-doped pressed pellets of 1,5-PNI have orders of magnitude larger dc conductivity than similarly doped PPI. The electrochemical oxidation results suggest that 1,5-PNI undergoes a greater degree of charge transfer on oxidation than the parent polymer PPI. However, the similarly reported higher dc conductivity of iodine-doped 1,5-PNI compared to a similarly doped PBPI[22] is not explained by our redox properties since PBPI and 1,5-PNI exhibit similar charge transfer characteristics under oxidation.

Electronic Structure. To further understand the electronic structure of this class of conjugated polymers it is essential to establish the relative positions of the characteristic electronic energy levels such as the high-

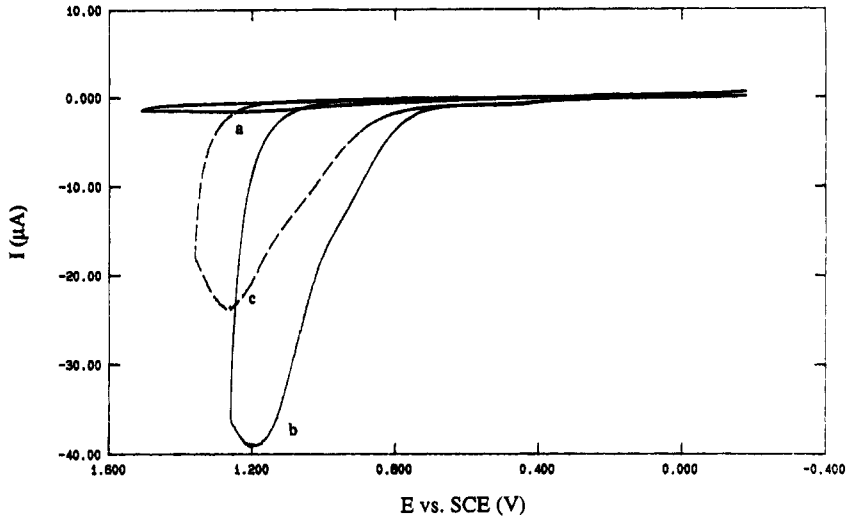

Figure 12. Cyclic voltammograms of the oxidation of PPI (a), PBPI (b), and PTPI (c) in 0.1 M $TBABF_4$ in acetonitrile.

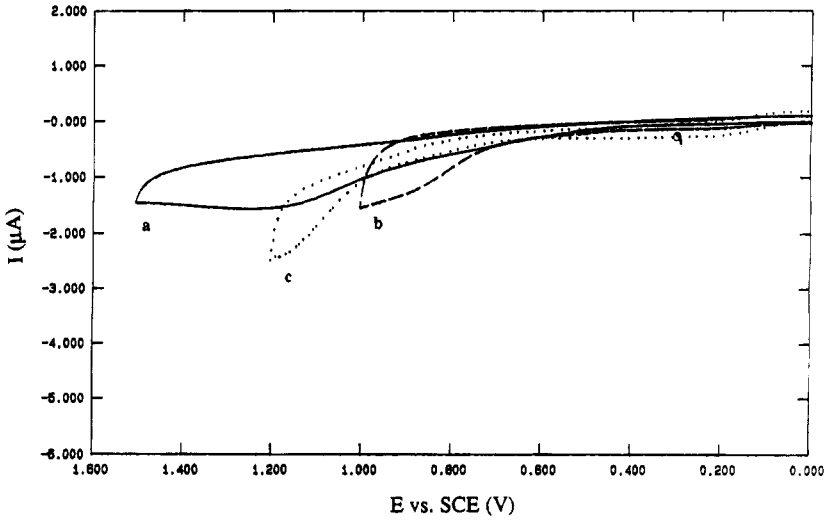

Figure 13. Cyclic voltammograms of the oxidation of PPI (a), PMOPI (b), and Cl_2-PPI (c) in 0.1 M $TBABF_4$ in acetonitrile.

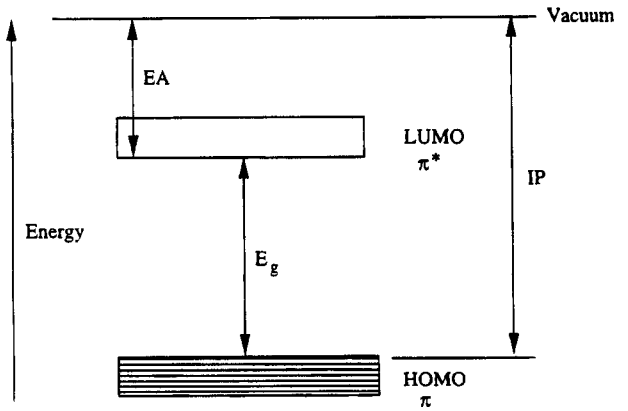

Figure 14. Schematic energy diagram of a conjugated polymer. Electron affinity (EA), ionization potential (IP), and LUMO-HOMO energy gap (E_g) are defined.

est occupied molecular orbital (HOMO or π level), the lowest unoccupied molecular orbital (LUMO or π^* level), and the associated energy parameters. Figure 14 is a schematic energy level diagram that defines the HOMO and LUMO levels relative to vacuum and three energy parameters: electron affinity (EA) which establishes the LUMO energy level; ionization potential (IP) which defines the HOMO energy level; and the LUMO-HOMO or $\pi-\pi^*$ energy gap E_g. The energy parameters EA and IP were estimated from the measured redox potentials on the basis of extensive prior work on conjugated polymers which has shown that:[50-53] $IP = E^{ox}_{onset} + 4.4$ and $EA = E^{red}_{onset} + 4.4$, where the onset potentials are in volts (vs SCE) and IP and EA are in electronvolts. The 4.4 eV constant in the relation between IP, EA, and redox potentials arises from the difference in gas-phase ionization potentials and electrochemical oxidation potentials of solid films and the solid-state polarization energy.[50-53] The LUMO–HOMO energy gap is obtained from the redox properties as $E^{el}_g = IP - EA = E^{ox}_{onset} - E^{red}_{onset}$. The IP, EA, and E^{el}_g values estimated from the electrochemical CVs as well as E^{opt}_g determined from the optical absorption spectra are collected in Table 8 for a series of 14 conjugated aromatic polyimines.

The electron affinity (EA) values of the 14 aromatic polyimines vary from 2.46 eV in PBPI (**4a**) to 2.94 eV in Cl_2-PPI (**3a**) (Table 8). This means that there is a 0.48 eV variation in EA and hence the LUMO energy level among the series of polymers. There is only a small reduction in electron affinity in going from PPI, the parent conjugated backbone polymer, to other backbone structures such as PSPI and 1,5-PNI and a slightly larger reduction in going from PPI to PBPI and PTPI. Side-group substitution causes the biggest changes in electron affinity relative to PPI. For example, there is a 0.34 eV increase in electron affinity by dichloro substitution on PPI and an increase of 0.15 eV by

Table 8. Electronic Structure Parameters of Conjugated Aromatic Polyimines

polymer	ionization potential[a] (IP) (eV)	electron affinity[b] (EA) (eV)	E_g^{el} (eV)[c]	E_g^{opt} (eV)
1a PPI	5.12	2.60	2.52	2.50
1b PMOPI	5.04	2.75	2.29	2.34
1c MO-PHOPI	5.00	2.74	2.26	2.07
2a MO-PPI	5.10	2.72	2.38	2.41
2b P3MOPI	4.97	2.73	2.24	2.23
2c MO-PHOPI	4.80	2.72	2.08	2.03
3a Cl_2-PPI	5.38	2.94	2.44	2.50
3b Cl_2-PMOPI	5.05	2.91	2.14	2.25
4a PBPI	5.19	2.46	2.73	2.50
4b PBMOPI	5.09	2.58	2.51	2.38
6a PTPI	5.26	2.49	2.77	2.58
6b PTMOPI	5.12	2.56	2.56	2.47
7a PSPI	5.06	2.55	2.51	2.38
8a 1,5-PNI	5.21	2.56	2.65	2.51
trans-polyacetylene[d]	4.73	3.31	1.42	1.53
poly(*p*-phenylene)[d]	5.42	2.58	2.84	2.80
poly(*p*-phenylene vinylene)[d]	5.11	2.71	2.40	2.34

[a] Determined from the onset oxidation potential. [b] Determined from the onset reduction potential. [c] Electrochemical gap E_g^{el} = IP-EA. [d] Data from refs 50, 52, 53, and 54.

dimethoxy substitution on PPI. Using the LUMO energy level of PPI as a reference, the polymer with the lowest lying LUMO (Cl_2-PPI) is 0.34 eV below PPI and PBPI which has the highest lying LUMO is 0.14 eV above PPI. The EA values of the aromatic polyimines are quite high compared to many other conjugated polymers except *trans*-polyacetylene which has an electron affinity of 3.31 eV (Table 8).[50] Again, these electron affinity values suggest favorable n-type dopability of this class of conjugated polymers to conducting polymers.

The ionization potential (IP) values (Table 8) determined from onset oxidation potentials for the series of aromatic polyimines vary from 4.80 eV in MO-PHOPI to 5.38 eV in Cl_2-PPI. This represents a 0.58 eV variation in IP and hence the position of the HOMO energy level. Among the series of polyimines, PPI with an IP of 5.12 eV has a HOMO energy that is 0.32 eV below the polymer with the highest lying HOMO (MO-PHOPI) and 0.26 eV above the polymer with the lowest lying HOMO (Cl_2-PPI). Polymer backbone variation among the aromatic polyimines generally results in an increase of the ionization potential relative to PPI, except PSPI (**7a**) which results in a slight decrease of IP value. Side-group substitution, on the other hand, generally results in a lowering of the ionization potential except in the dichloro derivative Cl_2-PPI. The ionization potential values of aromatic polyimines are to be compared with other well-known π-conjugated polymers such as *trans*-polyacetylene (4.73 eV),[50] poly(*p*-phenylene) (5.42 eV),[50] and poly(*p*-phenylenevinylene) (5.11 eV).[53]

The measured electrochemical LUMO–HOMO gap E_g^{el} was found to vary from 2.08 to 2.77 eV (Table 8), indicating a 0.69 eV variation with molecular structure in the series of polymers. A comparison of the electrochemical energy gaps with the optically measured LUMO–HOMO energy gaps E_g^{opt} shows a good agreement with a maximum deviation of 0.23 eV (or 8%) in PBPI.

The electronic structure parameters (EA, IP, and E_g) of Table 8 together with the previously discussed CV results provide a basis for assessing the conjugated aromatic polyimines as electronic, optoelectronic, electroactive, and photoactive materials as well as for comparisons with other conjugated polymers. For example, one sees the remarkable similarity between the electronic structures of PPI and poly(*p*-phenylenevinylene) (Table 8) which have isoelectronic molecular structures. The π-conjugated aromatic polyimines (Chart 1) have a range of ionization potentials and electron affinities which are accessible to conventional dopants for preparing electrically conducting polymers[1] or *ground-state charge transfer complexes*. In this regard, only p-type doping with iodine has previously been explored to date[19,22] but our electrochemical CV results suggest that n-type doping is not only feasible but probably more promising. We also point out that in the light of the recent discovery of *excited-state charge transfer complexes* of conjugated polymers,[6] the π-conjugated aromatic polyimines have a range of electronic structures that may be amenable to such excited state photoprocesses.

Conclusions

A systematically designed series of π-conjugated aromatic polyimines has been prepared and their molecular structures were characterized in detail. Although this class of polymers has been known and investigated for a long time,[10–22] it is only now that we have firmly established their molecular structures by a combination of solution ^{1}H NMR spectroscopy and FTIR and optical absorption spectroscopies of high quality thin films.

We have used optical absorption spectroscopy and cyclic voltammetry to explore the electronic structures of the π-conjugated aromatic polyimines in detail with the aim of shedding light on the effects of molecular structure and providing a basis for assessing the potential of this class of polymers as electroactive and photoactive materials. It was shown that, whereas the electrochemical reduction of the polyimines was reversible with good electron transfer (0.22 to 0.86 fractional charge transferred), oxidation was not reversible. Thus, although both p-type (oxidative) and n-type (reductive) doping of the polyimines are thermodynamically feasible, n-type doping appears to be more promising. The ionization potential, electron affinity, LUMO–HOMO energy gap, and redox potentials were correlated with the variation in backbone structure and side-group substitution. A novel feature of the aromatic polyimines compared to other conjugated polymers is that their electronic structures can be varied by backbone planarity regulation through *intramolecular hydrogen bonding* or Lewis acid complexation or diaryl phosphate complexation, in addition to the conventional variation through backbone structure and side-group changes.

Acknowledgment. This research was supported by the National Science Foundation (CTS-9311741), the NSF Center for Photoinduced Charge Transfer (Grant CHE-912-0001), the Office of Naval Research, and an Elon Huntington Hooker Fellowship to C.J.Y.

References and Notes

(1) (a) Aldissi, M., Ed. *Intrinsically Conducting Polymers: An Emerging Technology*; Kluwer Academic Publishers: Dordrecht, The Netherlands, 1993. (b) Bredas, J. L., Chance, R. R., Eds. *Conjugated Polymeric Materials: Opportunity in Electronics, Optoelectronics, and Molecular Electronics*; Kluwer Academic Publishers: Dordrecht, Holland, 1990. (c) Skotheim, T. A., Ed. *Handbook of Conducting Polymers*; Marcel Dekker: New York, 1986. (d) Bredas, J. L.; Silbey, R., Eds. *Conjugated Polymers: The Novel Science And Technology of Highly Conductive And Nonlinear Optically Active Materials*; Kluwer Academic Publishers: Dordrecht, The Netherlands, 1991.

(2) (a) Jenekhe, S. A. Ed. *Macromolecular Host-Guest Complexes: Optical, Optoelectronic, And Photorefractive Properties And Applications*. Materials Research Soc. Proceedings, 1992, Vol. 277. (b) Marder, S. R., Sohn, J. E., Stucky, G. D., Eds. *Materials for Nonlinear Optics: Chemical Perspectives*; American Chemical Society: Washington, DC, 1991. (c) Messier, J., Kajzar, F., Prasad, P. N., Ulrich, D. R., Eds. *Nonlinear Optical Effects in Organic Polymers*; Kluwer Academic Publishers: Dordrecht, The Netherlands, 1989.
(3) Burroughes, J. H.; Bradley, D. D. C.; Brown, A. R.; Marks, R. N.; MacKay, K.; Friend, R. H.; Burn, P. L.; Holmes, A. B. *Nature* **1990**, *347*, 539–541.
(4) Antoniadis, H.; Hsieh, B. R.; Abkowitz, M. A.; Jenekhe, S. A.; Stolka, M. *Synth. Met.* **1994**, *62*, 265–271.
(5) (a) Osaheni, J. A.; Jenekhe, S. A.; Perlstein, J. *Appl. Phys. Lett.* **1994**, *64*, 3112–3114. (b) Osaheni, J. A.; Jenekhe, S. A.; Perlstein, J. *J. Phys. Chem.* **1994**, *98*, 12727–12736.
(6) (a) Jenekhe, S. A.; Osaheni, J. A. *Science* **1994**, *265*, 765–768. (b) Osaheni, J. A.; Jenekhe, S. A. *Macromolecules* **1994**, *27*, 739–742.
(7) (a) Yang, C. J.; Jenekhe, S. A.; Vanherzeele, H.; Meth, J. S. *Chem. Mater.* **1991**, *3*, 985–988. (b) Meth, J. S.; Vanherzeele, H.; Jenekhe, S. A.; Roberts, M. F.; Agrawal, A. K.; Yang, C. J. *SPIE* **1991**, *1560*, 13–24. (c) Yang, C. J.; Jenekhe, S. A.; Vanherzeele, H.; Meth, J. S. *Mater. Res. Soc. Proc.* **1992**, *247*, 247–252. (d) Yang, C. J.; Jenekhe, S. A.; Vanherzeele, H.; Meth, J. S., in preparation
(8) (a) Agrawal, A. K.; Jenekhe, S. A.; Vanherzeele, H.; Meth, J. S. *Chem. Mater.* **1991**, *3*, 765–768. (b) Osaheni, J. A.; Jenekhe, S. A.; Vanherzeele, H.; Meth, J. S. *Chem. Mater.* **1991**, *3*, 218–221. (c) Jenekhe, S. A.; Osaheni, J. A.; Meth, J. S.; Vanherzeele, H. *Chem. Mater.* **1992**, *4*, 683–687. (d) Osaheni, J. A.; Jenekhe, S. A.; Vanherzeele, H.; Meth, J. S.; Sun, Y.; MacDiarmid, A. G. *J. Phys. Chem.* **1992**, *96*, 2830–2836. (e) Agrawal, A. K.; Jenekhe, S. A.; Vanherzeele, H.; Meth, J. S. *J. Phys. Chem.* **1992**, *96*, 2837–2843. (f) Vanherzeele, H.; Meth, J. S.; Jenekhe, S. A.; Roberts, M. F. *J. Opt. Soc. Am.* **1992**, *B9*, 524–533. (g) Jenekhe, S. A.; Roberts, M. F.; Agrawal, A. K.; Meth, J. S.; Vanherzeele, H. *Mater. Res. Soc. Proc.* **1991**, *214*, 55–59. (h) Chen, W.-C.; Jenekhe, S. A.; Meth, J. S.; Vanherzeele, H. *J. Polym. Sci.: Polym. Phys.* **1994**, *32*, 195–200.
(9) Yang, C. J.; Jenekhe, S. A. *Chem. Mater.* **1994**, *6*, 196–203. (b) Yang, C. J.; Jenekhe, S. A. *Chem. Mater.*, in press.
(10) (a) Yang, C. J.; Jenekhe, S. A. *Chem. Mater.* **1991**, *3*, 878–887. (b) Jenekhe, S. A.; Yang, C. J. U.S. Patent No. 5,236,980, Aug. 17, 1993.
(11) Adams, R.; Bullock, R. E.; Wilson, W. C. *J. Am. Chem. Soc.* **1923**, *45*, 521–527.
(12) (a) Steinkopf, W.; Eger, W. *Liebigs Ann. Chem.* **1938**, *533*, 270–279. (b) Steinkopf, W.; Leitsman, R.; Muller, A. H.; Wilhelm, H. *Liebigs Ann. Chem.* **1939**, *541*, 260–282.
(13) (a) Marvel, C. S.; Hill, H. W. *J. Am. Chem. Soc.* **1950**, *72*, 4819–4820. (b) Marvel, C. S.; Tarkoy, N. *J. Am. Chem. Soc.* **1957**, *79*, 6000–6002. (c) Marvel, C. S.; Bonsignore, P. V. *J. Am. Chem. Soc.* **1959**, *81*, 2668–2670.
(14) (a) D'Alelio, G. F.; Crivello, J. V.; Schoenig, R. K.; Huemmer, T. F. *J. Macromol. Sci.* **1967**, *A1*, 1161–1249. (b) D'Alelio, G. F.; Strazik, W. F.; Feigl, D. M.; Schoenig, R. K. *J. Macromol. Sci. Chem.* **1968**, *2*, 1457–1492. (c) D'Alelio, G. F. *Encyl. Polym. Sci. Technol.* **1969**, *10*, 659–670.
(15) Hodgkin, J. H.; Heller, J. *Macromolecules* **1969**, *2*, 556–558.
(16) (a) Morgan, P. W.; Kwolek, S. L.; Pletcher, T. C. *Macromolecules* **1987**, *20*, 729–739. (b) Morgan, P. W. U.S. Patent 4048148, Sep 13, 1977. (c) Morgan, P. W. U.S. Patent 4122070, Oct 24, 1978.
(17) Saegusa, Y.; Sekiba, K.; Nakamura, S. *J. Polym. Sci.: Polym. Chem.* **1990**, *A28*, 3647–3659.
(18) (a) Reinhardt, B. A.; Unroe, M. R. *Polym. Prepr.* **1990**, *31* (1), 620–621. (b) Reinhardt, B. A.; Unroe, M. R. *Polym. Commun.* **1991**, *32*, 85–87.
(19) (a) Lee, K. S.; Won, J. C.; Jung, J. C. *Makromol. Chem.* **1989**, *190*, 1547–1552. (b) Lee, K. S.; Samoc, M. *Polym. Commun.* **1991**, *32*, 361–362.
(20) Park, S.-B.; Kim, H.; Zin, W.-C.; Jung, J. C. *Macromolecules* **1993**, *26*, 1627–1632.
(21) (a) Mohite, S. S.; Wadgaonkar, P. P. *Polym. Prepr.* **1990**, *31* (1), 482–483. (b) Bryant, R. G. *Polym. Prepr.* **1992**, *33* (2), 182–183.
(22) Al-Jumah, K. B.; Wagener, K. B.; Hogen-Esch, T. E.; Musfeld, J. L.; Tanner, D. B. *Polym. Prepr.* **1989**, *30* (2), 173–174.
(23) Yang, H. H. *Aromatic High-Strength Fibers*; Wiley-Interscience: New York, 1989; pp 641–672.
(24) Wood, J. H.; Gibson, R. E. *J. Am. Chem. Soc.* **1949**, *71*, 393–395.
(25) Wood, J. H.; Tung, C. C.; Perry, M. A.; Gibson, R. E. *J. Am. Chem. Soc.* **1950**, *72*, 2992–2993.
(26) Burton, D. E.; Clarke, K.; Gray, G. W. *J. Chem. Soc.* **1965**, 438–443.
(27) Marx, J. N.; Song, P. S.; Chui, P. K. *J. Heterocyl. Chem.* **1975**, *12*, 417–419.
(28) Diaz, F. R.; Tagle, L. H.; Godoy, A.; Hodgson, C.; Olivares, J. P. *J. Polym. Sci.: Polym. Chem. Ed.* **1985**, *23*, 2757–2765.
(29) Yang, C. J.; Jenekhe, S. A. *Mater. Res. Soc. Symp. Proc.* **1992**, *277*, 197–204.
(30) Jenekhe, S. A.; Johnson, P. O. *Macromolecules* **1990**, *23*, 4419–4429.
(31) Roberts, M. F.; Jenekhe, S. A. *Polym. Commun.* **1990**, *31*, 215–217.
(32) Jenekhe, S. A.; Johnson, P. O.; Agrawal, A. K. *Macromolecules* **1989**, *22*, 3216–3222.
(33) (a) Roberts, M. F.; Jenekhe, S. A. *Chem. Mater.* **1990**, *2*, 224–226. (b) Roberts, M. F.; Jenekhe, S. A. *Chem. Mater.* **1990**, *2*, 629–631.
(34) Roberts, M. F.; Jenekhe, S. A. *Macromolecules* **1991**, *24*, 3142–3146.
(35) Beever, W. H.; Stille, J. K. *J. Polym. Sci.: Polym. Symp.* **1978**, *65*, 41–53.
(36) Agrawal, A. K.; Jenekhe, S. A. *Chem. Mater.* **1992**, *4*, 95–104.
(37) Agrawal, A. K.; Jenekhe, S. A. *J. Phys. Chem.*, submitted for publication.
(38) *CRC handbook of Chemistry and Physics*, 68th ed., CRC press: Boca Raton, FL, 1987; pp D151–D158.
(39) Gagne, R. R.; Koval, C. A.; Lisensky, G. C. *Inorg. Chem.* **1980**, *19*, 2855–2857.
(40) Millaud, B.; Strazielle, C. *Polymer* **1979**, *20*, 563–570.
(41) Aton, B.; Doukas, G.; Narva, D.; Callender, R. H.; Dinur, U.; Honig, B. *Biophys. J.* **1980**, *29*, 79–94.
(42) Lopez-Garriga, J. J.; Babcock, G. T.; Harrison, J. F. *J. Am. Chem. Soc.* **1986**, *108*, 7241–7251.
(43) Tieke, B.; Bubeck, C.; Leiser, G. *Macromol. Chem. Rapid Commun.* **1982**, *3*, 261.
(44) Burgi, H. B.; Dunitz, J. D. *J. Chem. Soc., Chem. Commun.* **1969**, 472–473.
(45) Traetteberg, N.; Hilmo, I.; Abraham, R. J.; Ljunggren, S. *J. Mol. Struct.* **1978**, *48*, 395–405.
(46) Maeda, K.; Muszkat, K. A.; Sharafi-Ozeri, S. *J. Chem. Soc., Perkin Trans. 2* **1980**, 1282–1287.
(47) Odian, G.; Yang, N.-L.; Wei, Y. *Magn. Reson. Chem.* **1985**, *23*, 908–915.
(48) Yang, N.-L.; Odian, G.; Wei, Y. *Polym. Mater. Sci. Eng.* **1986**, *55*, 481–485.
(49) Rudzinski, W. E.; Gutherie, S. R.; Cassidy, P. E. *J. Polym. Sci.: Polym. Chem.* **1988**, *26*, 1677–1680.
(50) Frommer, J. E.; Chance, R. R. *Encyl. Polym. Sci. Eng.* **1985**, *5*, 462–507.
(51) Miller, L. L.; Nordblom, G. D.; Mayeda, E. A. *J. Org. Chem.* **1972**, *37*, 916–918.
(52) Bredas, J. L. In ref 1c, pp 859–913.
(53) Eckhardt, H.; Shacklette, L. W.; Jen, K. Y.; Elsenbaumer, R. L. *J. Chem. Phys.* **1989**, *91*, 1301–1315.
(54) McCoy, R. K.; Karasz, F. E. *Chem. Mater.* **1991**, *3*, 941–947.

MA9411787